ABSTRACT

Title of Document: A NEW OPTICAL TECHNIQUE FOR PROBING CLEAR AIR TURBULENCE

Joseph D. Harris, Ph.D. 2011

Directed By: Christopher C. Davis, Professor, Department of Electrical and Computer Engineering

A new optical technique for probing the small scales turbulence has been developed. When light is transmitted through the atmosphere, it can scatter off vortex filaments in the air that are at different densities from the surrounding air, and hence, have different indices of refraction. These filaments, or eddies are distributed through a turbulent flow. Our experiment illuminated a turbulent flow with an expanded Gaussian laser beam. Two detectors, capable of translation perpendicular to the beam path, observed intensity fluctuations at different points. By analysis of two point spatial transmission correlation functions, the smallest length scales of clear air turbulence can be determined in real time without disturbing the flow. By changing the type of air flow, different length scales associated with different conditions have been measured optically. The measured scales agree with measurements done by hotwire techniques and correspond to the Kolmogorov microscale.

A NEW OPTICAL TECHNIQUE FOR PROBING CLEAR AIR TURBULENCE

By

Joseph Daniel Harris

Dissertation submitted to the Faculty of the Graduate School of the
University of Maryland, College Park, in partial fulfillment
of the requirements for the degree of
Doctor of Philosophy,
2011

Advisory Committee:
Professor Christopher Davis, Chair
Professor Mario Dagenais
Professor Thomas Cohen
Professor Edward Redish
Professor Robert Anderson

Dedication

Rabbi Eliezer the son of Shamua would say: The dignity of your student should be as precious to you as your own; the dignity of your colleague, as your awe of your master; and your awe of your master as your awe of Heaven.

- Pirkei Avot, Ch. 4:12

There are many good people who deserve profound gratitude for helping me to get to this point, but I must thank my teacher and mentor, Chris Davis first. Thank you for believing in me, encouraging me when needed, and most importantly, sharing your time, knowledge and expertise with me. I do not have adequate words to express my thanks. I thank Bob Gammon for sharing his experimental insights. I thank every professor I have had at the University of Maryland for teaching me so much. Special thanks must go to Jim Gates, who taught me strings, Tom Cohen, who taught me Jackson and so much else with humor and intelligence, Joe (I still hope to someday find out where he got Joe from) Redish, who taught me how to teach, and Jim Wallace, who taught me how to do hotwire anemometry. I thank everyone in the Maryland Optics Group, who have all been good friends and wonderful colleagues.

My loving and dedicated family can never be thanked enough. Mom, Dad, Sharon, David and Debbie, are the best family anyone could hope for. Zack, Vivian, Yaakov, Devara, Scott, Ehren and Dave are all like siblings to me. They deserve to be mentioned here.

Finally, I must thank Emily, who made thesis writing something to smile through. This work is dedicated with gratitude, to all of these people.

Table of Contents

List of Tables

List of Figures

Introduction

This work introduces a new experimental method for probing the smallest scales in atmospheric turbulence. What began as an exploration into the effects of atmospheric (or clear air) turbulence on the transmission of optical signals became a direct probe into the small structures of fluid turbulence itself using optical techniques. There are many advantages of this method. It is very accurate and produces robust results in real time. It does not disturb the flow in any way. It does not require tracer particles or other means of decorating the flow. It is comparatively easy to deploy and use (in comparison to hotwire anemometry or particle imaging velocimetry) and it is inexpensive to construct the actual equipment. Unlike previous work on optical transmission through fluid turbulence, which was done at long range, where light was transmitted through a very wide interaction region producing multiple scatterings and interferences, this work was done at short range where the light was assumed to only scatter once from a structure in the turbulent flow. Due to this, it was possible to investigate the structures of the flow itself.

This work has three major parts. The first part covers a basic overview of the theory and phenomenology of fluid turbulence and a brief discussion of the optics relevant to the problem of light transmission through fluid turbulence. The fluid theory reviewed is quite mature and can be found discussed in many excellent textbooks, seminal papers and review articles. However, it was essential to include this discussion in order to justify the main claims of the experimental results, namely that the optical device developed detected features of fluid turbulence that were to be

expected for the flows under consideration. It was essential to present enough information to give the reader an intuitive sense for the behavior of fluid turbulence and some of the difficulties its study presents. The experimental nature of this work demanded that the goal of this section was to include only as much theory as was needed to discuss the experiment. Due to this, many interesting discussions about the theory of fluid turbulence, like the "road to turbulence" and the relationship of the theory to chaos were completely omitted. Only passing reference was made to many fascinating (and even some basic) topics from a very rich discipline. By no means is the theoretical discussion of fluid turbulence meant to be comprehensive nor does it represent any sort of theoretical breakthrough.

The theoretical discussion of optics is similarly limited. Most theoretical work done in the past involving optical transmission through turbulence involved long range radar, communications or astronomical applications. Typical scales were on the order of kilometers or higher. This work applies to an entirely different optical regime; ray optics, over short distances on scales less than a meter. Almost none of the previous theoretical work in the field applies. It should be pointed out that since the hotwire probe is the workhorse of many fluid turbulence experiments, almost none of the previous experimental work into studying the scales of turbulence apply either, other than as a check to make contact with what has been observed in turbulent flows before. In this sense, this work is both interdisciplinary and unique.

The second part of this work contains the experimental details of this project. It discusses the design, construction and operation of the experimental device itself.

Experiments were also performed with hotwire anemometry. A brief discussion of hotwire anemometry is also included in this section.

The third major section of this work reviews the results and discusses measurement of errors. The goal of this section is not only to demonstrate what was observed by the technique, but to point out that what was observed was what would be expected from the theoretical basics of fluid turbulence. It is not claimed that this new device is seeing anything new yet. It is claimed that it is seeing exactly what should be seen in a new way that is reliable, fast, and does not disturb the flow under observation. Further, this technique zeros in on the very smallest scales of fluid turbulence preferentially so it gives a direct look at the scales which are dissipating mechanical energy to heat through viscosity. It can distinguish different flows from the change in that scale from one flow to another. It produces results in real time without the need for elaborate post processing. One can observe the correlation functions "settle" in a matter of minutes. In principle, the entire system could be automated and all analysis which is currently done post process could be done by coding additional software. Once the system is aligned, there is no difficult calibration needed. With a higher bit resolution, one could get accurate measurements in tens of seconds. By comparison, hotwire probes take in all scales at once, they must be calibrated individually, they must be placed into the flow itself, and they are extremely temperamental, fragile and expensive.

Chapter 1: An introduction to fluid basics and the challenges of turbulence

Setting the stage

This work started as an investigation of how fluid turbulence in the air effects the transmission of optical signals. This is a multidisciplinary subject that bridges both optics and fluid mechanics. The fruit of this labor was the development of an instrument that can probe structures in clear air turbulence. This chapter will attempt to lay out some of the basics of turbulence from a theoretical view. By no means is this an attempt to be an exhaustive discussion of a very rich field. Rather, the goal of this chapter is to lay out sufficient theory to justify the experimental claims made later.

Turbulence, as might be inferred from the title of this chapter, is a very complex subject that presents many challenges both theoretically and experimentally. Studying turbulence requires working with turbulent flows and demands developing familiarity with different flows. While that last statement may seem obvious, in this context, it means that the mathematics is such that one must use a heuristic and phenomenological approach in attacking these sorts of problems. There is certainly

hard and fast physics to be discussed and solid physical principle to be understood, however, unless one is dealing with one of a few special cases, the theory is more of a guide to developing proper intuition of how these systems behave than something that can be solved explicitly. This is because the ultimate underlying theory of turbulence, the Navier-Stokes equations, can not, in general, be solved explicitly and computer modeling of its solutions in a given case is severely restricted by computing power. For solid mathematical reasons, much of the discussion of turbulence must revolve around scaling arguments and phenomenology.

This chapter will lay out what some of those problems are in a more rigorous fashion and discuss some of the things that we can actually say solidly about the issues. We start by laying out some of the basics of fluid mechanics and discuss some of the theoretical issues behind exploring the phenomena of turbulence. As an example of the difficulties of this subject, it is important to note that there is no universally accepted definition of what exactly turbulence is. It is a mark of the complexity of the subject that turbulence is very much something that one knows when one sees it. This problem is further compounded by the fact that when a fluid dynamacist talks of turbulence, what is meant is a certain state of a fluid system, while in the optical world, what is meant is something that is done to an optical signal passing through fluid turbulence. These are two very different things even if the optical papers frequently use them synonymously. Sometimes in this field, the problem is not only seeking the correct answers, but perhaps even having the correct questions.

We have from our everyday experience, an intuitive sense of what turbulence is. We can picture rapids in a stream, or the complex patterns in billowing smoke. It is as if any notion of smooth flow or graceful streamline has been utterly banished – and yet there seem to be patterns within patterns. A precise mathematical discussion of what qualifies as turbulence, and when a system has stopped transitioning into turbulence from a smooth flow and actually becomes a fully turbulent state is something that is discussed at length and debated in the literature. Ultimately that is a discussion of a transition into chaos and a detailed discussion of that issue is beyond the scope of this work. For the sake of discussion in this work, our turbulence is already fully developed and fully developed turbulence is defined as a state of statistically isotropic fluid motion where the analysis of Kolmogorov applies. Kolmogorov's ideas will be discussed and outlined in this chapter. One can also approach these ideas by looking at vorticity. One goal of this chapter will ultimately be to refine what is meant by turbulence and some of its basic properties in the context of the flows examined. In so doing, this will justify later claims that the new instrument sees exactly what one would expect it to see.

As a first brush, turbulence is a highly complex and dissipative state of fluid motion. It is chaotic in the mathematical sense of the word, and much of the beginnings of chaos theory started with problems associated with turbulence and fluid flows. As such, if one were to perform a fluid turbulence experiment, even the tiniest deviation in initial conditions would generate a completely different realization of turbulence, and any theory of turbulence that would be based on tracking one realization of it, i.e., something that could deterministically follow the evolution of

one fluid element, would be essentially useless – in much the same way that tracking an individual molecule of gas in a cylinder would be useless to describing what the gas was doing as a whole. Much like the case in statistical mechanics, only certain bulk and average features of turbulent flows can be discussed. Any theory of turbulence must therefore be statistical in nature. Turbulence is very much like entropy in the sense that, there are a number of ways to discuss it, but putting it into non-mathematical language that gives a true picture of what it actually is can be very difficult. Unlike entropy however, we do not have any neat definitions of it to be written as simple (or even not so simple) mathematical expressions.

Much of the background in this chapter can be found in many standard (and excellent) fluid mechanics texts. However, since the overall work presented in this thesis is very interdisciplinary, it is worth including the fundamentals. I follow the discussions of Landau, Davidson, Tartarski and Hinze [1,2,3,4] to present the basics.

A brief note on notation

Unfortunately, in the field of fluid mechanics, and the literature of optical problems associated with transmission through turbulence, one encounters a wide variety of differing notations and notational legacies. This problem is further complicated by the fact that much of fluid mechanics has developed its own notational traditions which may be confusing to someone who specializes in a different field. These issues go beyond something like the different conventions of a mostly minus metric vs. a mostly plus metric when employing relativistic transformations. For example, sometimes η, will be the dynamic viscosity, and other times, it will be the Kolmogorov microscale, which some optics papers refer to as l_0.

Other optics papers define l_0 as the Taylor microscale, while fluid mechanics papers use λ. In some fluid papers, λ sometimes also means thermal conductivity. All optics papers refer to l_0 (reserving λ for wavelength) as the "inner scale" of turbulence; though sometimes, it is unclear which small turbulent scale is being referred to exactly at all! What each of these things are will be discussed in due course.

As a result of this, great care has been taken to be explicit about notation throughout this text, and the text will consistently follow one set of fluid mechanics notational conventions. Even so, out of the necessity of legacy, sometimes, the same notation will be used to denote radically different things. The reader is urged to examine the context of any given expression when in doubt, and they should especially do so, should they develop an interest in the wider literature. Equation Chapter 1 Section 1

The basics of fluid mechanics

The first and most basic notion of fluid mechanics is the notion of a fluid element. A fluid element is a vanishingly small volume of the fluid that is small enough to be treated as a differential, yet contains enough atoms or molecules of the fluid that it is not necessary to take the behavior of individual atoms or molecules into account. In some sense, a bulk parameter of a fluid that contains an "average" of molecular properties is viscosity.

One could ask at what point the equations of fluid mechanics, which are written in terms of fluid elements, would break down – and they would, for a

sufficiently rarified gas or, sufficiently small enough scale of observation. However, for air at one atmosphere and around room temperature, or for that matter, most fluid experiments, this presents no difficulty. At the scales and densities germane to this writing (air, at close to one atmospheric pressure and sub-millimeter scales) this is not an issue. Using the Ideal Gas Law, $PV=nRT$, to estimate the number of molecules in a cubic mm of air, under laboratory conditions, gives on the order of 2×10^{15} molecules and an average separation distance on the scale of nanometers. More importantly, the mean free path is on the scale of tens of nanometers. Intuitively, the mean free path must be the lowest bound on the applicability of the notion of a fluid element because any element smaller than that, would have some fraction of its constituent particles constantly leaving the element.

The fluid element is treated in a way somewhat analogous to the way that charges are treated in classical electromagnetism. Mathematically, there are many similarities between the fundamentals of fluid mechanics and classical electromagnetism. Both are completely classical vector field theories. Both subjects were investigated and developed by many of the same people. Many of the manipulations one would employ when examining Maxwell's equations carry over to the discussion of fluids as well. Unlike Maxwell's equations however, the Navier – Stokes equations present a substantially greater mathematical challenge.

To properly begin our discussion, we consider a volume of space V, which contains a fluid of density ρ. The total mass of fluid contained in V must be:

$$\int \rho dV$$

The flow of mass out of V per unit time must be:

$$-\frac{\partial}{\partial t}\int \rho dV$$

However, the flow of mass out of a volume V can also be represented by:

$$\oint \rho \mathbf{u} \cdot d\mathbf{n}$$

Where **u** is the velocity of a fluid element and d**n** is a unit vector along the outward normal over the surface that encloses V. Equating these two expressions is nothing more than saying that mass is conserved.

$$-\frac{\partial}{\partial t}\int \rho dV = \oint \rho \mathbf{u} \cdot d\mathbf{n} \tag{1.1}$$

The right hand side of (1.1) can be converted to a volume integral and the partial derivative on the left can be carried through. This gives us

$$\int \left[\frac{\partial \rho}{\partial t} + \nabla(\rho \mathbf{u}) \right] dV = 0$$

for any arbitrary volume element. For this integral to always vanish, the expression in brackets must vanish. This is the equation of continuity. Expanding, the equation of continuity is given by

$$\frac{\partial \rho}{\partial t} + \rho \nabla \cdot \mathbf{u} + \mathbf{u} \cdot \nabla \rho = 0 . \tag{1.2}$$

Later, we will argue that the assumption that $\nabla \cdot \mathbf{u} = 0$ is justified in many cases, however if we assume that our fluid is homogenous and has a constant density, this condition immediately follows.

So far, we have not taken viscosity or "fluid friction" into account. A fluid that does not take these things into account is called an ideal fluid. It is instructive to discuss an ideal fluid briefly, by deriving Euler's equation (of fluids) before complicating matters.

Using vector analysis, we can consider the effects of pressure gradients on the fluid element. If we consider the pressure field p applied to a fluid element and then integrate it over the surface of that element we can convert to a volume integral in terms of ∇p. Imbalances in p create a net force on our fluid element. However, the fluid element is not static. In order to express the instantaneous effect of these gradients on the element, the mathematics must describe a co-moving frame. We can immediately write:

$$\rho D\mathbf{u}/Dt = -\nabla p \tag{1.3}$$

where we use mass per unit volume instead of mass to write force per unit volume.

The clever part of this derivation comes from asking what exactly is meant by $D\mathbf{u}/Dt$ when we are actually discussing a fluid element that is itself moving along with an overall fluid flow. This notation is not an accident. It denotes a derivative that follows the fluid element around as it moves in the overall flow. This is called the convective derivative and it was first introduced by Stokes. We construct it via the chain rule. For a scalar, A, moving in the flow, we would simply write:

$$\delta A = (\partial A/\partial t)\delta t + (\partial A/\partial x)\delta x \tag{1.4}$$

Switching to the case at hand, we have, over some time interval dt, two parts that we need to analogously evaluate for the vector quantity **u.** The first is $(\partial \mathbf{u}/\partial t)dt$ which is calculated relative to an arbitrary fixed point in space. The second part is the spatial variation of the fluid element away from that fixed point. This is given for a vector by writing $dx\dfrac{\partial \mathbf{u}}{\partial x} + dy\dfrac{\partial \mathbf{u}}{\partial y} + dz\dfrac{\partial \mathbf{u}}{\partial z}$. Dividing by dt, we obtain the convective derivative of **u**,

$$D\mathbf{u}/Dt = \partial\mathbf{u}/\partial t + (\mathbf{u}\cdot\nabla)\mathbf{u}\,. \tag{1.5}$$

Which automatically gives upon substituting (1.3)

$$d\mathbf{u}/dt + (\mathbf{u}\cdot\nabla)\mathbf{u} = -\frac{1}{\rho}\nabla p\,. \tag{1.6}$$

Convective derivatives are defined as $D(\cdot)/Dt = \partial\mathbf{u}/\partial t + (\mathbf{u}\cdot\nabla)(\cdot)$ where $(\cdot)$ is a place holder for whatever the convective derivative is operating on, and **u** is the overall local flow of the fluid. Convective derivatives follow the usual rules of differentiation.

Equation (1.6) is Euler's equation of fluid mechanics, which is an equation of motion for a fluid element in the absence of viscosity. Again, ρ is density and p is pressure. If one wanted to add a term for gravity acting on the fluid, all one needs to do is multiply through by ρ and add ρg to the right hand side of the equation.

It is very important to note the $(\mathbf{u}\cdot\nabla)\mathbf{u}$ term in Euler's equation. By following a very straight forward set of ideas, the fundamental non-linearity of fluid mechanics arises almost instantly and with very little effort. It is fundamentally impossible to escape non-linearity if one accepts the notion of a fluid element, very basic Newtonian physics and basic vector calculus. Mathematically, this non-linearity is the source of many beautiful things – indeed all of turbulence - because it will turn out that the equations of fluid mechanics would be very well behaved without it and nothing like a turbulent flow could possibly arise. However, Euler's equation is of limited use. Real fluids are generally dissipative in their motions because they have the property of viscosity.

The next step is to form the Navier – Stokes equations, which take viscous effects into account and appends them to Euler's equation. Ultimately, the conceptual idea behind viscosity is analogous to friction. Fluids with high viscosity, like honey or tar, flow slowly and mix with great difficulty. They are difficult to move through. Viscosity is something that is dissipative of both momentum and energy. It arises when two fluid elements are in contact with each other and move relative to each other. Ultimately, viscosity comes from the molecular or atomic structure of the fluid itself; however, there is no need to look into it with that degree of detail here. If we visualize this, we can easily imagine that the effect of such a property might be to apply shear stresses to a fluid element. Let us continue to assume that ρ is a constant. This implies that we are dealing with an homogenous fluid of uniform density. If we assume that our fluid element is instantaneously in the shape of a cube, we can begin to write expressions for these forces. Just to be careful in our discussion, force here is in terms of density and not mass.

We start by simply noticing that whatever these viscous forces are must add on to the end of the Euler equation and note they must comprise both shear forces and normal forces acting on our instantaneously cubical fluid element. This gives us nine quantities to worry about, and is best written in tensor notation. We adopt the tensor τ_{ij} for this purpose. All indices run over *x*, *y* and *z*. In such notation, τ_{xy}, τ_{yz}, τ_{zx} etc… are the shear stresses and τ_{xx}, τ_{yy} and τ_{zz} are the normal forces. The notation τ_{xy} means that the force is in the *x* direction relative to a plane normal to *y*. Since we are not looking at relativistic fluids, the time component is treated as a separate entity.

Any net imbalance in these stresses τ_{ij} will lead to net acceleration of the fluid element. For example, a difference in τ_{xy} between the top and the bottom of the element would produce a net acceleration in the *x* direction. So we must be looking for changes in *x* as we vary from top to bottom in *y*. To get the total effect, we need to integrate over the whole element and collect terms. We find that a net viscous force in the *j* direction, f_j is given by

$$f_j = \frac{\partial \tau_{ij}}{\partial x_i} \delta V \tag{1.7}$$

where summation over repeated indices is understood. This allows us to immediately write a more full equation of motion.

$$\rho \, d\mathbf{u}/dt + (\mathbf{u} \cdot \nabla)\rho\mathbf{u} = \rho \frac{D\mathbf{u}}{Dt} = -\nabla p + \frac{\partial \tau_{ij}}{\partial x_i} \tag{1.8}$$

Multiplying through by ρ on the tensor term of (1.8) was left out with malice aforethought. It will be put back in as we refine what that term means.

To get more detail, we invoke Newton's law of viscosity. Stresses and strains will deform our fluid element. Newton's law of viscosity simply postulates that the stress and strain be proportional to the density of the fluid, a constant ν (which is called the kinematic viscosity) and the rate of change of velocity of the fluid element in a given direction. In other words, as the element drags along, getting "rubbed" by other viscous fluid elements it slows down more the further it goes. Newton clearly sees viscosity as bleeding energy out of the fluid element. We collect all possible terms in a given direction and write

$$\tau_{ij} = \rho\nu\left(\frac{\partial u_i}{\partial x_j} + \frac{\partial u_j}{\partial x_i}\right). \tag{1.9}$$

Substituting (1.9) into (1.8) we obtain the Navier-Stokes equation.

$$\rho\, d\mathbf{u}/dt + (\mathbf{u}\cdot\nabla)\rho\mathbf{u} = \rho\frac{D\mathbf{u}}{Dt} = -\nabla p + \rho\nu\nabla^2\mathbf{u} \tag{1.10}$$

If we wish to add a gravity term or any other force term to the equation of motion, we just add it on to the right hand side as before with Euler's equation. The Navier Stokes equation is the "fundamental theory" of fluid mechanics. It is non-linear and non-local.

It turns out that one can relate pressure to velocity. This has profound consequences. If we assume a constant density and take the divergence of both sides of (1.10) we are left with

$$\nabla\cdot(\mathbf{u}\cdot\nabla)\mathbf{u} = -\nabla^2\left(\frac{p}{\rho}\right) \tag{1.11}$$

Equation (1.11) is invertible via the Biot-Savart law over an infinite domain.

$$p(\mathbf{x}) = \frac{\rho}{4\pi}\int\frac{[\nabla\cdot(\mathbf{u}\cdot\nabla)\mathbf{u}]'}{|\mathbf{x}-\mathbf{x}'|}d\mathbf{x}' \tag{1.12}$$

The implication is that we can write pressure at a point in space in terms of velocity if we know the velocity field over all of space. However, that means that the velocity field over all of space contributes to the pressure at a given point. This is what is meant by the statement that the Navier-Stokes equations are non-local. Physically, the condition $\nabla\cdot\mathbf{u} = 0$ implies that sound waves travel infinitely fast or that the fluid is incompressible. Even if we relax that condition and allow for sound waves to travel at some large speed relative to the scales we are looking at, and further

complicate the terms of the Navier – Stokes equations, we would still find that the pressure at any given point still depends on what its neighbors are doing out to some radius. At the end of the day, any structure of the fluid communicates with all other structures in the flow, and those structures change and communicate back to the original part of the fluid under consideration.

The next step is to discuss how viscosity dissipates energy in a fluid flow. We start with a definition.

$$S_{ij} = \frac{1}{2}\left(\frac{\partial u_i}{\partial x_j} + \frac{\partial u_j}{\partial x_i} \right) \tag{1.13}$$

This is called the strain rate tensor and we see from the definition that

$$\tau_{ij} = 2\rho\nu S_{ij} \tag{1.14}$$

We can construct an energy equation or more specifically, a rate of change of energy equation out of (1.10) by dotting both sides with the field **u.** Noting that

$$\mathbf{u} \cdot \frac{D\mathbf{u}}{Dt} = \frac{D}{Dt}\left(\frac{u^2}{2} \right)$$

After much algebra, we receive

$$\frac{\partial\left(u^2/2\right)}{\partial t} = -\nabla\cdot\left[\left(u^2/2\right)\mathbf{u}\right] - \nabla\cdot\left[\left(p/\rho\right)\mathbf{u}\right] + \frac{\partial}{\partial x_j}\left[u_i\tau_{ij}/\rho\right] - 2\nu S_{ij}S_{ij} \tag{1.15}$$

where

$$\frac{\partial}{\partial x_j}\left[u_i\tau_{ij}\right] = \frac{\partial\tau_{ij}}{\partial x_j}u_i + \tau_{ij}\frac{\partial u_i}{\partial x_j}$$

and the operator ∇ is understood to act as a gradient or a divergence as appropriate.

This is an equation that tells how the energy in the fluid changes with time. If we imagine the fluid enclosed by an arbitrary boundary, the four terms in (1.15) are identified as follows [2]:

1. The rate of kinetic energy convected across a boundary
2. The work done by pressure on the boundary
3. The work done by viscous forces on the boundary
4. The loss of mechanical energy to heat.

From this, we identify that the rate of dissipation of mechanical energy to heat, ε is given by

$$\varepsilon = 2\nu S_{ij} S_{ij} . \tag{1.16}$$

One could follow a similar derivation by taking the cross product of **u** and (1.10) on both sides to show

$$\varepsilon = 2\nu S_{ij} S_{ij} = \nu \left(\nabla \times \mathbf{u} \right)^2 . \tag{1.17}$$

Immediately, we see that the dissipation of mechanical energy to heat in a flow has something to do with the curl of the flow. Automatically, a curl invokes an image of some form of rotation and a curl of the velocity field invokes some sort of swirling motion. Swirling motions in fluids are given many names. In this work, eddies and vortices are used interchangeably for that purpose. From equation (1.17) we see that vortices dissipate energy to heat through viscosity. The picture will soon emerge that turbulent flows have many scales of motion that cascade down, by passing energy through ever smaller scales and ultimately give up their energy to heat through viscosity at the smallest scales. With this in mind, we define the vorticity field, $\boldsymbol{\omega}$ as

$$\boldsymbol{\omega} = \left(\nabla \times \mathbf{u} \right) \tag{1.18}$$

Though it may seem a bit of mathematical slight of hand, we can decompose any velocity gradient into a strain component and a vorticity component.[1,2]

$$\frac{\partial u_i}{\partial x_j} = \frac{1}{2}\left(\frac{\partial u_i}{\partial x_j} + \frac{\partial u_j}{\partial x_i}\right) + \frac{1}{2}\left(\frac{\partial u_i}{\partial x_j} - \frac{\partial u_j}{\partial x_i}\right) = S_{ij} - \frac{1}{2}\varepsilon_{ijk}\omega_k \tag{1.19}$$

From its mathematical form, we can see that vorticity is properly named. The velocity field through the strain tensor S_{ij} will deform a fluid element, or push it along, and the vorticity ω will rotate it. Considering this in terms of the entire velocity field intuitively shows the mathematical origins of swirling motions in fluids. Vorticity stacks in much the same way that one can picture magnetic fields being formed out of adding magnetic moments. It becomes appropriate to talk about vortex tubes and lines of vorticity in a flow. It is these structures that our experiment is observing.

The origin of vorticity in a given flow frequently turns out to be an interaction with a boundary layer or a physical boundary. For example, when a flow goes through a pipe, or wind interacts with a solid object, viscosity causes the flow to rub against the boundary which imposes a torque. These torques create vortex tubes which are then blown along by the main flow.

In order to discuss how vortex tubes evolve, and discuss a little more about vorticity itself, we can, with some work, manipulate the Navier Stokes equation (1.10) into the following form.

$$\frac{D\boldsymbol{\omega}}{Dt} = \left(\boldsymbol{\omega}\cdot\nabla\right)\mathbf{u} + \nu\nabla^2\boldsymbol{\omega} \tag{1.20}$$

This is accomplished by taking a curl and using a vector identity for $\nabla\left(u^2/2\right)$.

The first term of the right hand side of equation (1.20) generates stretching of the

vortex tube while the second term diffuses vorticity through the fluid. This can be seen by noting that if one neglects the first term on the RHS, we have a diffusion equation. From this, we can see that once vorticity starts, it diffuses through the medium. We note in passing, that if we were to restrict ourselves to only two dimensions, the first term would disappear automatically, since $\boldsymbol{\omega}$ would always be perpendicular to the divergence of **u.** Because of this, discussions of two dimensional flows are fundamentally different than three dimensional ones for more than just the obvious difference in dimensionality.

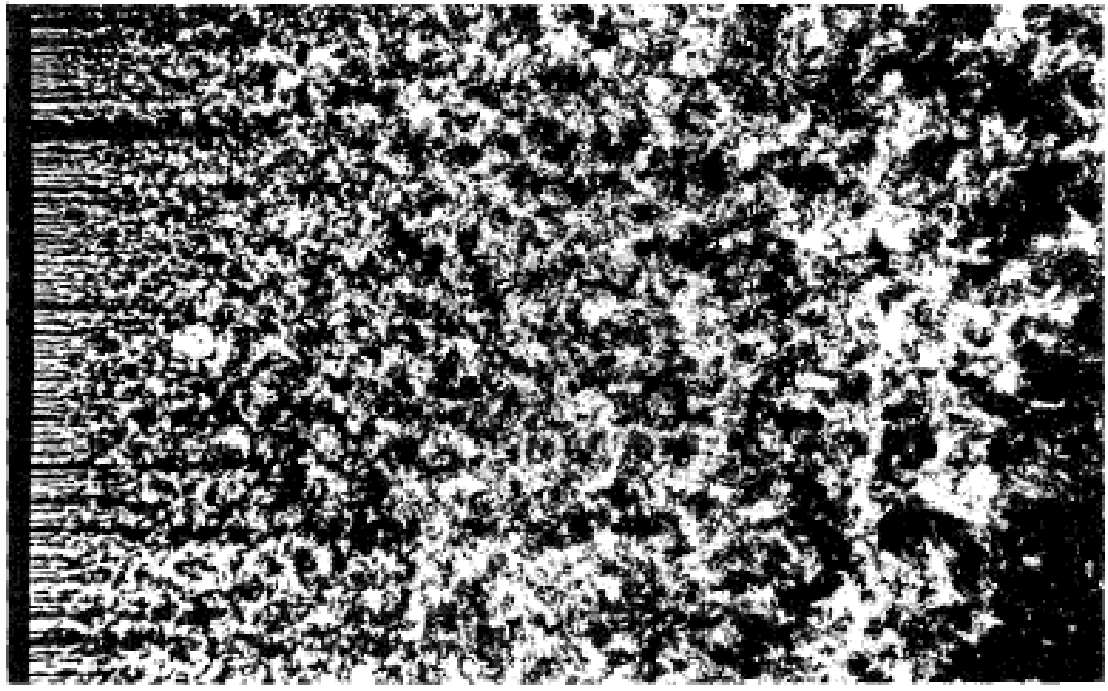

Fig [1.1] An image of the evolution of grid turbulence from Tsinober [5] p.14. Smoke has been added to air to act as a tracer. The diffusion of vorticity through the flow is plainly visible as the flow evolves.

As stated above, the effect of the first term of (1.20) is to stretch vortex tubes. This is readily seen by imagining a vortex tube and a set of coordinates defined along

it. If we define a coordinate *s* along the length of the tube, and u_s as a velocity component in that direction, we see immediately that $(\boldsymbol{\omega}\cdot\nabla)u_s = |\boldsymbol{\omega}|\,du_s/ds$. If du_s/ds is positive, then two arbitrary points along *s* would move apart and the vortex tube would be stretched. In order to conserve angular momentum, this would make the vorticity increase which we see readily by referring back to (1.20). However, as vorticity increases, by equation (1.17) energy dissipation increases. The walls of the vortex tube are a lossy boundary layer that can generate other motions. This happens all the way down to a scale where viscous forces dominate and give up the energy of vorticity to heat through viscosity. Once a tube is stretched too thin, it "evaporates."

We can now justify the picture that a turbulent flow has many scales of motion that exchange energy in a cascade. Large scales rub against boundary layers and bleed energy off into smaller scale vortices. This goes down to a range of smallest scales where the kinetic energy of the motion is quickly turned into heat. The existence of these many scales of motion corresponding to many scales of vorticity is familiar to anyone who has watched leaves swirl on a windy day or watched patterns of smoke coming from a cigarette. There are cycles within cycles. Using Kelvin's theorem, we can discuss how these cycles get moved along with the overall flow.

Kelvin's theorem applies to the special case that viscosity is zero. Obviously viscous effects are very important – as shown above to the evolution of real world fluids. However, for very many fluids of interest, like air, in the case of this experiment, viscosity is very small, and even though the theorem does not apply directly, it is still instructive to examine. Lord Kelvin showed via his theorem (stated without proof) that for an inviscid fluid vortex lines become frozen into the flow. It

will be shown that high Reynolds number flows correspond to turbulent flows and the limit of zero viscosity. This is because of the definition of the number, and the fact that as the Reynolds number increases, the non-linear terms of the Navier-Stokes equations dominate. Even though no real fluid commonly encountered is inviscid, the limit of zero viscosity corresponds to a state of "pure" turbulence. It is therefore still instructive to discuss Kelvin's theorem.

Mathematically, we wish to look at the rate of change in flux of the solenoidal field $\boldsymbol{\omega}$ through a material surface *S*. A material surface means that it is composed of the same fluid particles, and the whole thing is moving along with the flow. It turns out that [2] p.48:

$$\frac{d}{dt}\int_S \boldsymbol{\omega}\cdot d\mathbf{S} = \int_S \left[\frac{d\boldsymbol{\omega}}{dt} - \nabla\times(\mathbf{u}\times\boldsymbol{\omega})\right]\cdot d\mathbf{S}\,. \tag{1.21}$$

But for an inviscid flow,

$$\frac{d\boldsymbol{\omega}}{dt} = \nabla\times(\mathbf{u}\times\boldsymbol{\omega})\,. \tag{1.22}$$

Therefore,

$$\frac{d}{dt}\int_S \boldsymbol{\omega}\cdot d\mathbf{S} = 0\,. \tag{1.23}$$

Clearly, the integral part of (1.23) is a constant with respect to time. We can convert to a line integral over the bounding curve of the surface and arrive at a formal statement of Kelvin's theorem.

$$\Gamma = \oint \mathbf{u}\cdot d\mathbf{l} \tag{1.24}$$

where Γ is a constant called the circulation. What this means is that the circulation is conserved in an inviscid fluid as the flow evolves. This implies physically that the

vortex lines in a fluid move with the flow as if they are frozen into the flow. This an elegant mathematical way of saying that we expect to see tubes of vorticity move down stream. If we take viscostiy into account, we see that these tubes of vorticity give up their energy as they evolve. That evolution and the nature of turbulence phenomenologically, is the topic of the next sections.

The work of Reynolds

One thing that can not be overstated when discussing turbulence is a certain respect for clearly stating upfront those things which can not be stated clearly. This is not meant as joke, but rather an admission of the limitations imposed upon us by the difficulties of working with the Navier-Stokes equations, whose unknown solutions are deeply sensitive to initial conditions, and which must also change according to different boundary conditions. The tantalizing intuitive insights into the behavior of fluids one can garner from manipulating the equations through vector analysis techniques, statistical assumptions and the creation of non-dimensional parameters provide a strong phenomenological picture of the system in general terms. However, they leave room for some arbitrariness in the application of certain definitions. None the less, on the level of physical intuition about such systems, these insights are invaluable.

Before discussing Kolmogorov's statistical insights into turbulence, it is very instructive to discuss the work of Reynolds. While many physical systems can be successfully analyzed, by taking one limit or another that effectively linearizes the equations, turbulent flows were observed by Reynolds to arise from the non-

linearities of the Navier-Stokes Equation. In the Nineteenth century, Reynolds did a number of experiments involving the flow of water in pipes. His experiments varied flow rates and pipe diameters. He characterized these flows with, his now well known, non-dimensional number $\mathrm{Re} \equiv lu/\nu$, where *l* is the diameter of the pipe and *u* is the overall flow rate. The literature also frequently denotes the Reynolds number by *R*. When Reynolds did his experiments, he observed that above a certain critical value of Re, the flow in the pipes became turbulent. Consider the steady state form of the NSE,

$$(\mathbf{u}\cdot\nabla)\mathbf{u} = -\frac{1}{\rho}\nabla p + \frac{\eta}{\rho}\nabla^2\mathbf{u}. \tag{1.25}$$

The term η is called the dynamic viscosity and its notation is a legacy. It must not be confused with the Kolmogorov microscale, which is unfortunately, frequently denoted in the literature, by the same Greek letter. In this context, the kinematic viscosity is related to the dynamic viscosity by $\nu = \frac{\eta}{\rho}$. Notice that dimensionally, $\frac{\eta}{\rho}\nabla^2\mathbf{u} \sim \eta u/\rho l^2$ is linear in $\mathbf{u}$, and that $(\mathbf{u}\cdot\nabla)\mathbf{u} \sim u^2/l$ is non-linear. Here, *l* is a characteristic length scale that Reynolds associated with the largest possible scales of vortices, and hence, with the diameter of the pipe. Eventually, in the discussion of Kolmogorov's ideas, a value of *l* defined in such a manner, will become an example of an outer scale of turbulence. The ratio of the terms is

$$\frac{(\mathbf{u}\cdot\nabla)\mathbf{u}}{\frac{\eta}{\rho}\nabla^2\mathbf{u}} \sim \frac{u^2/l}{\eta u/\rho l^2} = \frac{ul}{\nu} = \mathrm{Re}. \tag{1.26}$$

This means that for small Re, the nonlinear term of the Navier Stokes equation is negligible, and the equations become approximately linear and very much better behaved. We immediately see several things from the definition of the Reynolds number. A fluid with high viscosity effectively dampens non-linearities and as a result, highly viscous, slowly flowing fluids like tar or honey do not easily (if ever!) give rise to turbulence. This should also make sense in the context of equation (1.20) and the discussion that followed it. Vorticity diffuses through the velocity field with viscosity as the coefficient. A high viscosity therefore causes vortices to diffuse and dissipate rapidly with respect to space, and such motions to very rapidly give their energy over to heat with respect to time.

On the other hand, in the limit of zero viscosity, Re explodes, which would be equivalent to a state of "pure" turbulence, and the phenomenology of Kelvin's theorem becomes very relevant. A fluid with low viscosity, like air or water, guarantees that vorticity can propagate through the medium, interact with other centers of vorticity and generate the complex and unpredictable (in a non-statistical sense) flows observed in turbulence.

The Reynolds number marks a transition into turbulence. This is exactly what Reynolds observed as he increased the rate of flow while he kept the pipe diameter fixed. Beneath a certain critical value, streamlines are smooth, and above it, turbulence is to be expected. In practice, turbulence develops in pipe flows for Reynolds numbers around 3000 depending on experimental conditions and how one defines l, the characteristic large scale of the system. For a circular pipe, the diameter is the logical choice for l, but suppose, one has a square or rectangular pipe. Suppose

one wanted to discuss the flow around an object moving through a fluid? In practice, *l* becomes the hydraulic diameter, which is defined as four times the cross sectional area of the pipe or object divided by wetted perimeter, which is the perimeter of that area which is in contact with the fluid. With a pipe this reduces to the diameter.

Exactly where the critical number lies depends on the geometry of the flow, the boundary conditions involved and the definitions used. The Reynolds number on the one hand, is an insightful guide for when to expect turbulence, but on the other, it is impossible to produce a hard and fast universal constant for the critical value.

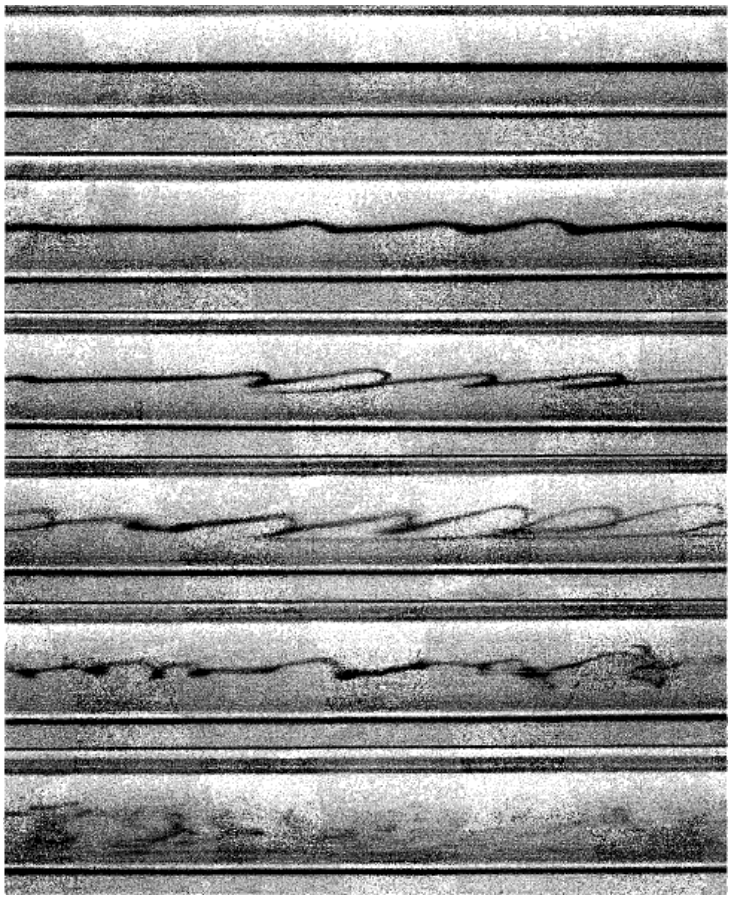

Fig [1.2]. A pipe flow experiment. Ink is injected into the fluid to visualize the flow. Successive experiments are shown as one goes down the photo. Moving downwards, the flow rate and hence, R increases.[5]

There is also a turbulent, or Taylor, Reynolds number. Which is denoted R_λ .

$$R_\lambda = \frac{\lambda \bar{u}}{\nu} \tag{1.27}$$

where λ is the Taylor scale (to be defined later, but represents a small scale at which eddies begin to dissipate to viscosity), and $\bar{u}$ is the deviation of the mean of the fluid velocity. From this definition, it is clear why this is called a turbulent Reynolds number. The deviation of the mean of the velocity field represents a velocity associated with smaller structures added on to the speed of the overall flow, and the Taylor microscale is the scale at which those smaller structures begin to go to viscosity. The advantage of R_λ is that it characterizes a local level of turbulence without having to make assertions about the outer scale or the history of the turbulence.

In the field of fluid mechanics, there are many other nondemsional numbers that have been developed to characterize fluid flows. Two other such numbers, which will become relevant to the discussion of hotwire anemometery, are The Prandtl number and the Nusselt number. The Prandtl number is used to characterize heat flows, and is the ratio of the viscous diffusion rate to the thermal diffusion rate.

$$\mathrm{Pr} = \frac{\nu}{\alpha} = \frac{c_p \eta}{k_f} \tag{1.28}$$

Here, $\alpha = k_f / \rho c_p$ is the thermal diffusion rate, c_p is the specific heat, and k_f is the thermal conductivity, with units of *W/mK*, and is not to be confused with the

Boltzman constant. When one remembers that the effect of viscosity is to bleed off energy from fluid motion, one sees that a small Prandtl number means that heat diffuses very quickly compared to loss of energy due to viscosity. Air, at one atmosphere, has a small Prandtl number of around 0.7. We note in passing, that the Peclet number is the mass transfer analogue of the Prandtl number.

The Nusselt number, Nu, is the ratio of conductive heat transfer to convective heat transfer.

$$Nu = \frac{hl}{k_f} \tag{1.29}$$

Here *h*, is the convective heat transfer, *l*, is the characteristic length (as in the definition of the Reynolds number) and k_f is the thermal conductivity of the fluid.

It should be mentioned that all of the non-dimensional numbers and scales discussed form not only a rule of thumb reference for conditions in a complicated flow, but also create sanity check for the experimentalist. They are something better than being able to "just" extract "something" from a complicated flow that can be used as a touch stone. If for instance, one has in hand, a reasonable estimate of Re being 2, it is unlikely that there is any turbulence. If Re is well over 3000, one can rest assured that there is fully developed turbulence somewhere. However, they all very much do arise (and particularly in the case of discussing different commonly used turbulent scales) from the need to be able to "just extract something" which is still meaningful to be spoken about, and measurable by someone else, from the data.

The ideas of Kolmogorov

The great Russian mathematician and physicist, A.N. Kolmogorov is credited with some of the deepest insights into the theory of turbulence. His approach to the problem was almost entirely statistical in nature. His insight was to impose the symmetries of the Navier Stokes equations onto his statistical description and to then impose phenomenological arguments.

The symmetries of the Navier-Stokes equations are:

$$(t,r,v)\mapsto(t,r+r',v)\quad r'\in\mathbb{R}^3 \tag{1.30}$$

$$(t,r,v)\mapsto(t+\tau,r,v)\quad \tau\in\mathbb{R} \tag{1.31}$$

$$(t,r,v)\mapsto(t,r+ut,v+u)\quad u\in\mathbb{R}^3 \tag{1.32}$$

$$(t,r,v)\mapsto(t,-r,-v) \tag{1.33}$$

$$(t,r_i,v_i)\mapsto(t,\mathbf{A}_{ij}r_i,\mathbf{A}_{ij}v_i)\quad \mathbf{A}_{ij}\in SO(3) \tag{1.34}$$

$$(t,r,v)\mapsto(\lambda^{1-h}t,\lambda r,\lambda^h v)\quad \lambda\in\mathbb{R}_+\ h\in\mathbb{R}\lim_{\upsilon\to 0} \tag{1.35}$$

In words, the symmetries are space and time translation, Galilean transformation, parity, rotation, and scaling. One thing that should leap out is the scale symmetry (1.35). In the limit of zero viscosity, one sees different scales as a symmetry of the equations and hence, a feature of the system. This is immediately reminiscent of the turbulent energy cascade. The different scales are identified with the multiple different vorticity structures, or eddies, in the flow [6].

Observationally, as was discussed earlier, as Re increases, flows begin to break these symmetries. In fully developed turbulence, the visible symmetries of

lower Re flows are completely absent. Since there are such tremendous mathematical difficulties surrounding turbulence, searching for statistical properties of turbulence becomes natural if not essential. Even if it were possible to calculate, knowing the full trajectory of a given fluid element for one realization of turbulence would not be particularly helpful (in of itself) in discussing what is going on in another realization of turbulence.

This leads to the next major (some say the deepest [6]) insight into turbulence by Kolmogorov.[8,9] Kolmogorov combined statistical methods with phenomenology and observation to write his landmark papers on turbulence during the Second World War. The Kolmogorov picture must be developed in several steps.

Implicit in his papers, is the hypothesis that the symmetries of the NSE return *in a statistical sense* in a state of fully developed turbulence. He set out to define statistics with the assumptions of homogeneity and isotropy and went on to impose all of the symmetries. By homogeneous he meant that the statistics are independent of time and position translations, and by isotropic he imposed that the statistics are both rotation and parity invariant.

Kolmogorov was certainly aware of the phenomenology of turbulence in terms of the energy cascade. He was also well aware that at the smallest scales, vortices would dissipate to heat. This led Kolmogorov to postulate the existence of an inner and an outer length scale for turbulent flows. The outer scale, L is the length scale at which energy is injected into the system. In pipe flows, the obvious choice for L is the diameter of the pipe, since it is not possible for there to be any larger scale of motion. If vorticity diffuses from the walls, it can only ever diffuse as far as the

other wall of the pipe. It is the size of the largest possible eddies produced. Those large eddies cascade their energy down through the smaller scales. The inner scale l_0 is the scale that viscous effects take over, and energy of motion is converted into heat. In between these scales is what is called the inertial convective range – so named because this represents the vortices which are being blown down stream as per the discussion of Kelvin's theorem. The phenomenology of looking in this range is the next piece of his model.

We define ε as energy dissipation per unit mass i.e. it has units of $J/s \cdot kg$.

Consider an eddy or vorticity structure, smaller than the outer scale, but still large enough that viscous effects do not destroy it. It has some characteristic length scale of *l*. If we eliminate ν from our considerations, because we are looking at fully developed turbulence, where viscosity goes to zero, the only physical parameters of a fluid left to express ε are ρ, u, the overall flow velocity, and l, the scale of the eddy or vortice. On purely dimensional grounds, Kolmogorov argued

$$\varepsilon \sim u^3 / l \tag{1.36}$$

$$u_l \sim \varepsilon^{1/3} l^{1/3} \text{ and } t_l \sim l^{2/3} \varepsilon^{-1/3} \tag{1.37}$$

where the subscript *l* is a reminder that we are talking about a vortex or eddy that is of a given scale *l*. From this we see a characteristic turnover time and eddy velocity.

The turnover time is interpreted as a lifetime for a given eddy at a given scale before is spawns other vortices or dissipates. This is related to the energy dissipation which Kolmogorov postulated was scale invariant. In other words, he postulated that the energy flowed down to the lower scales at the same rate.

On the other hand, one could consider the viscous regime, where diffusion takes over, and again argue on purely dimensional grounds that

$$t_{diss} \sim l_{diss}^2 / \nu . \tag{1.38}$$

This gives a timescale for the dissipation (which is what the subscript *diss* denotes). The two time scale expressions cross. Equating the two time scales, and solving for the characteristic dissipation length gives η (which is not to be confused with dynamic viscosity, this is a notational legacy) the Kolmogorov micro scale. The Kolmogorov microscale represents an "average value" for the smallest possible turbulent scales.

$$\eta \equiv \left(\nu^3 \diagup \varepsilon \right)^{1/4} \tag{1.39}$$

One immediately sees from this definition, that as viscosity gets smaller, it becomes possible to make smaller and smaller scales. One also sees that as the energy available for the cascade increases, it is possible to "push through viscosity" to ever smaller scales. On the flip side, if ε is small, and it depends on *u*, the dissipation scale could easily be larger than the outer scale of the system. To make this concrete, for a small pipe flow *u*, the turbulent energy cascade never gets started. This is a neat little sanity check that the phenomenology agrees with observation.

It is very important to note that in air, the time scales associated with the length scales in the inertial convective range, $\eta < l < L$, are much longer than the time it would take sound to cross an eddy. This is the justification for assuming incompressibility.

We are now in a position to put the bits together and look at Kolmogorov's statistics. In his first paper [8] (referred to in the literature as K1941a) Kolmogorov started with a general expression for a two point velocity correlation function. He then imposed the constraints of homogeneity and isotropy and converted to spherical coordinates. He does this in the context of the structure function $D_v(r_1, r_2)$ which is intimately related to the correlation function and is defined as (in modern notation)

$$D_u(r_1, r_2) = \left\langle [\mathbf{u}(r_1) - \mathbf{u}(r_2)]^2 \right\rangle \tag{1.40}$$

where $\langle \bullet \rangle$ denotes statistical averaging. In the context of isotropy and homogeneity, the structure function becomes a function of $\Delta r \equiv r$ only. Kolmogorov ultimately imposes Eq.(1.33) and makes the following predictions:

$$B_{rr}(r) = D_u(r) = C\varepsilon^{2/3} r^{2/3}, \quad \eta < r < L \tag{1.41}$$

$$B_{tt}(r) = \tfrac{4}{3} B_{rr}(r), \quad \eta < r < L \tag{1.42}$$

$$B_{rr}(r) = \tfrac{1}{15} \varepsilon r^2 / \nu, \quad r < \eta \tag{1.43}$$

where η, the microscale and C is a constant. B_{rr} and B_{tt} are the longitudinal and transverse components of the two point correlation function.

The two thirds law, Eq.(1.37) is of great importance to scattering from turbulent flows. Kolmogorov's third paper from 1941 [9] is of great importance to turbulence theory directly. He makes the same statistical assumptions and scaling arguments, but instead, started by examining the three point correlation function and found that he could draw conclusions directly from the NSE themselves. He predicts

$$\left\langle (\delta v(r))^3 \right\rangle = -\tfrac{4}{5} \varepsilon r \quad \lim_{\mathrm{Re} \to \infty} \mathrm{Re} \tag{1.44}$$

where $\left\langle (\delta v(r))^3 \right\rangle$ is a convenient notation for the three point velocity correlation function. Eq. (1.40) is of such importance because it is exact and non-trivial. It imposes a sort of "outer limit" on any possible theory of turbulence in that any such theory must either obey (1.40) or break one of its assumptions.

At this point, we pause in our discussion to define what we mean by turbulence in the context of this work. We mean that turbulence is a highly dissipative state and chaotic state of fluid flow, where multiple scales of motion exist and cascade energy down to dissipation through viscosity, and the ideas of Kolmogorov apply. That is to say, that there is a sufficiently high Re, the turbulence is fully developed and isotropic.

One might reasonably complain that all of this discussion has been little more than a phenomenological discussion of turbulence based on clever rearrangements of the Navier-Stokes equations and appeals to physical intuition. It may seem like little more than a parlor trick. The insights of Kolmogorov frankly are little more than imposing symmetries and phenomenology onto basic tensor algebra. As such, they are arguably somewhat divorced from the system in question.

It is certainly true that much more theoretical development investigating the Navier- Stokes equations has been done than is presented here, and that turbulence theory is a very large, active and fruitful field [7]. However, it is always reduced to noticing and elucidating the phenomenological features or the rich mathematical features of the Navier-Stokes equations as they apply to this or that set of constraints or conditions coupled with a strong measure of physical intuition. This applies to all cases. We can discuss the general behavior of certain families of solutions to these

equations, in certain circumstances, but we can only talk about turbulence in such phenomenological terms. Unfortunately, this is the best that can be done. This is because we have no way as yet to solve the equations directly. If we could somehow solve for the velocity field given a set of initial conditions then there would be nothing left to do with the theory. The Navier-Stokes equations are too compellingly generated from basic physical principles to expect (or hope!) that something else will come and replace them.

Many great physicists and mathematicians have tried to attack the equations directly for over a century. None have succeeded, though many have shed light on various facets of the problem. No general solution as yet has been found. The mathematics necessary to make a successful attack might not yet even exist. It has been said in many texts, that many believe that there will never be an overall theory of turbulence, but rather a collection of specific theories for specific flows under specific conditions. All is not lost however. We can still sufficiently describe and predict many behaviors of turbulent flows with what we have.

Some final notes on turbulent scales

The statistical analysis of the Navier-Stokes equations lends itself very well to the study of correlations of the velocity field. From this analysis, two additional scales are commonly discussed. These are the integral scale and the Taylor microscale. Both of these scales are usually measured with hotwire probes.

The integral scale is the area under a time auto-correlation curve for the velocity field, which was transformed into a spatial correlation by multiplying with the local flow speed. The correlation function is dimensionless. The area under the curve takes on units of length. Since the smaller scales are more numerous than the larger scales, this corresponds to a weighted average measure of all turbulent scales in the system. It is of necessity smaller than the outer scale.

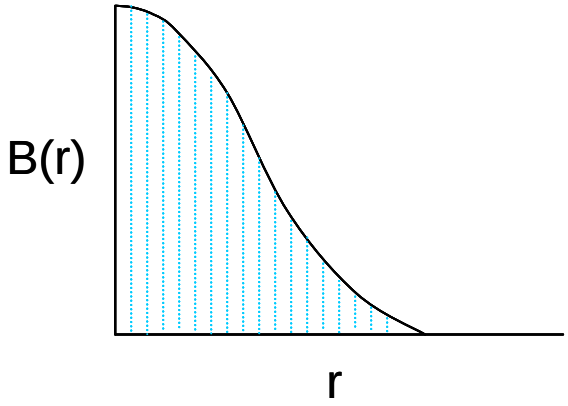

Fig[1.3]The Integral Scale is the area under a spatially transformed time autocorrelation function. This has units of length since B(r) is dimensionless.

The Taylor microscale, λ is created by taking the first two terms of a Taylor expansion of the spatially converted time autocorrelation. Those two first terms correspond to a parabola which must intersect the x axis. The x intercept of that parabola is the Taylor microscale. Phenomenologically, $\lambda \sim \mathrm{Re}^{-1/2} l$. It can be thought of as the scale where loss of kinetic energy to viscosity begins to take effect.

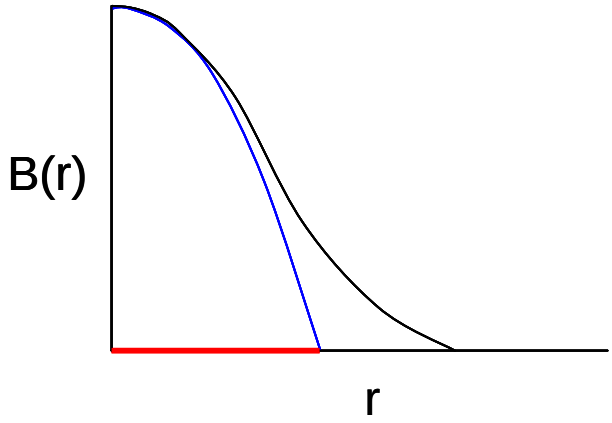

Fig [1.4] The Taylor microscale is the x intercept of the first two terms of a Taylor expansion of a correlation.

As a final remark on phenomenology, there are three statistical results that are useful for analyzing hotwire anemometry data which are presented here without derivation [2].

$$\eta = (\nu^3 / \langle \varepsilon \rangle)^{1/4} \tag{1.45}$$

$$\langle \varepsilon \rangle = 15\nu \left\langle (\partial u / \partial x)^2 \right\rangle \tag{1.46}$$

$$\lambda = \left[\langle u^2 \rangle / \left\langle (\partial u / \partial x)^2 \right\rangle \right]^{1/2} \tag{1.47}$$

In all of these expressions, $\langle u^2 \rangle^{1/2}$ is the root mean square velocity fluctuation.

Important points in summary:

1. The Navier - Stokes equations contain the theory of turbulence.
2. As the Reynolds number increases, the non-linear terms in the Navier-Stokes equations become significant.

3. This leads to many different scales of motion in turbulence which are characterized by vorticity.
4. The larger scales exchange energy to smaller scales by spawning them.
5. This process continues down to the inner scale, where the interaction of vorticity and energy dissipation converts kinetic energy into heat.
6. The greater the initial flow speed and hence Re, the smaller the smallest scales are.
7. There are several commonly used and measurable scales of turbulence that are discussed. Going from largest to smallest, they are the outer scale, the integral scale, the Taylor scale and the Kolmogorov microscale. The outer scale represents the scales at which energy is injected into the system. The integral scale is formally the area under a velocity correlation function curve (hence integral). It represents a sort of average scale somewhere in the inertial range. The Taylor scale is extracted by taking the x intercept of the first two terms of a Taylor expansion of a velocity correlation function. This represents the point that scales begin to die off due to viscosity. The Kolmogorov microscale is extracted phenomenologically and is the scale where viscosity must dominate.

Some notes on the correlation function

Since the research presented in this work revolves around measurements of correlation functions, a discussion of them is in order. In this work, we define the correlation function as follows

$$B(d) = \left\langle \frac{\Delta I_A(d)\Delta I_B(0)}{\sigma_A \sigma_B} \right\rangle \tag{1.48}$$

where $\Delta I = I - \langle I \rangle$, subscripts *A* and *B* refer to channels A and B, σ is the deviation, and brackets refer to averaging. In the experiment, the correlations of two voltages, which correspond to intensity, are measured. This is a discretized form of the correlation. The parameter (d) is the separation in either space or time, depending on context, of either the actual physical separation of the two detectors, or the lag in time between samplings. When $d = 0$ we refer to that as the autocorrelation, and it implies that $I_A = I_B$. To be very specific, in terminology, this is the demeaned, two point, cross correlation of discrete samples of signal A and signal B. "Two point" means that it convolves two signals that it accepts as arguments. One could define higher order, *n*-point correlation functions involving *n* quantities, or define them in a continuous case which would accept functions for the arguments and then integrate. However, there is no need to consider such cases here.

The correlation function *B(d)* is a statistical function, which on average, is bounded on the interval [1,-1]. It tells of a dependence or a relationship between the two arguments in a statistical sense. If the correlation is 1, the two quantities being fed into the correlation function are said to be perfectly correlated. In other words, this is a measure of the two things being the same thing. If the correlation is zero, the signals are said to be uncorrelated. This is a way of saying that the two inputs have no statistical relation to each other at all. This implies that there is no relationship at all between what is going on at B compared to what is going on at A. If it is -1 then the signals are said to be anticorrelated. This implies that whenever signal A is doing one

thing, signal B is always doing a specific other thing. One can see from the definition that *B(0)* always equals 1.

Before remarking further on the mathematical properties of the correlation function, it is important to point out that a measured correlation function is model independent. One role of theory may be to attempt to explain why this sort of correlation as opposed to that sort of correlation obtains. However, one need not know anything about the particular signals one is analyzing to determine if there is a correlation between them. As an experimental technique, in the sense of something that is useful to measure, this makes the correlation function very powerful. An analysis of the correlation function will determine if two signals correspond to looking at the same thing, and how long or how far apart the sources of the signals must be before they are looking at something else. This makes the correlation function an obvious choice to probe scales in a turbulent flow. The scales must relate to how long it takes a correlation function to de-correlate.

Some mathematical properties of the correlation function are:

$$B(d) = B(-d) \tag{1.49}$$

and

$$\left|B(d)\right| \le B(0)\,. \tag{1.50}$$

The way that discrete correlation functions increase sensitivity through demeaning is seen as follows. Let us compare a non demeaned correlation function to a demeaned one. Brackets will represent averaging and summation over indices, as always, is implied. We define the non normalized correlation as:

$$\left\langle A_i B_i \right\rangle \tag{1.51}$$

And we define

$$\Delta A = A_i - \bar{A} \quad \Delta B = B_i - \bar{B} \tag{1.52}$$

where the bar also represents taking a mean average. This is of course simply the demeaned variable. Then

$$A_i = \Delta A + \bar{A} \tag{1.53}$$

and an identical expression can be made for B_i. Substituting these expressions into (1.51) we obtain the following:

$$\langle A_i B_i \rangle = \langle \bar{A}\bar{B} + \Delta A\bar{B} + \Delta B\bar{A} + \Delta A \Delta B \rangle \tag{1.54}$$

Since we expect ΔA and ΔB to have an equal chance to be above or below the means of A and B respectively for any given data point, we expect the long term average of these quantities to vanish. Also, since averaging commutes with addition (1.54) reduces to

$$\langle A_i B_i \rangle = \langle \bar{A}\bar{B} \rangle + \langle \Delta A \Delta B \rangle \tag{1.55}$$

as i gets large. What we see from this is that the demeaned correlation is something that sits on top of a large constant (the product of the averages) in the undemeaned correlation. If one is dealing with small fluctuations in comparison to the average signal, the interesting part of the expression, where all the data is, can get lost. Since, in our experiment, the average received voltage was on the order of 1V, and the standard deviation of the fluctuations was on the order of 0.001V, which is very small in comparison, using the de-meaned correlation was a necessary step to extract the data of interest.

It can be seen from the definition, that the demeaned correlation function can become negative. It is possible for a given reading to fluctuate below the mean. Theoretical work by Fante predicts negative portions of the correlation in certain cases of optical transmission through turbulence [29].

Optics and Scattering

Doing an optical experiment to measure the scales of turbulence fluctuations could not be possible if light did not interact with the turbulence fluctuations themselves. It is well known that atmospheric fluctuations interfere with the transmission of optical signals. Most people have seen the way that images waver when looking over hot asphalt or the stars twinkling at night. Signals can be broken up, scattered, or caused to wander off a target in numerous ways. This is of particular importance if one is interested in radar or using adaptive optics for optical telescopes in astronomy, for example. Most of the literature in the optics world revolves around attempting to overcome the issue of getting a clean optical signal through atmospheric "noise." Atmospheric effects from multiple scatterings and interferences can create a very complex speckle-like pattern in the incoming light. The results of this are very dramatic. A wave front that started smooth and Gaussian becomes a complicated speckle-like pattern.

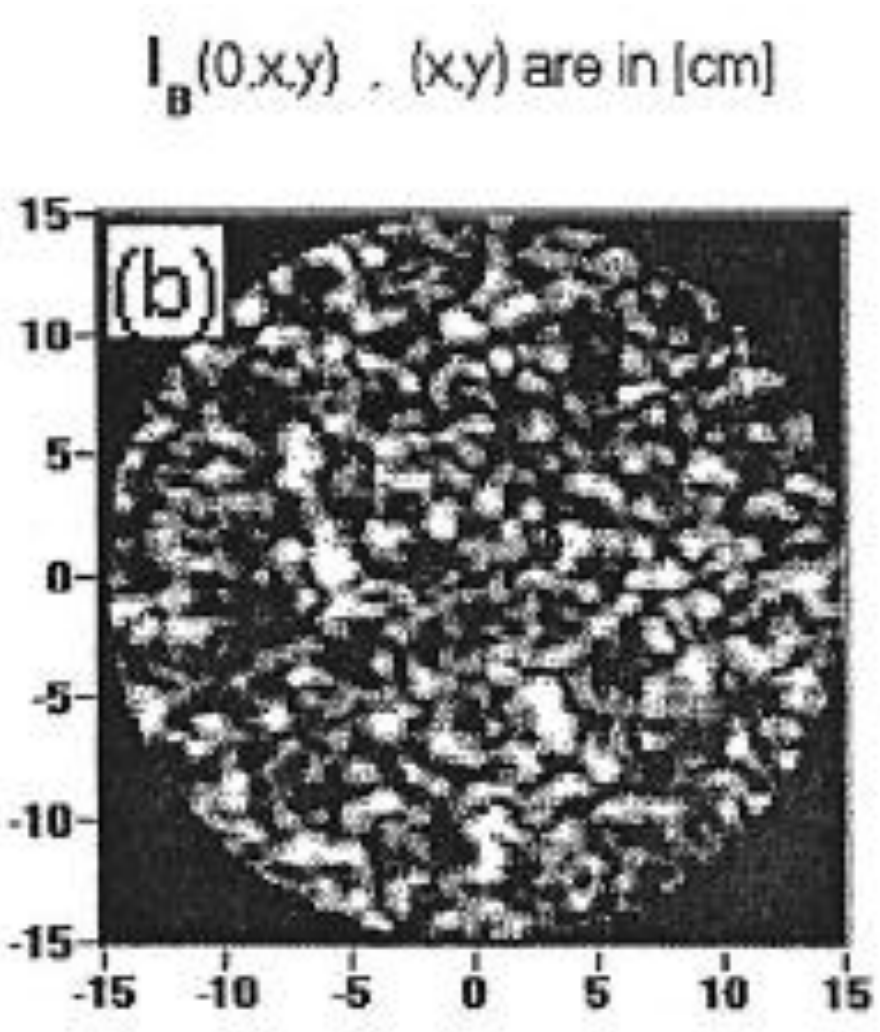

Fig[1.5] A picture of the intensity variations of laser light, taken over long range after interacting with atmospheric turbulence, to produce optical turbulence. The scale is in cm. Reproduced from Banakh et al.[13] By contrast, the flutuations measured our experiment, are not visible to the naked eye.

Since the current experiment studies scattering of short wavelength light that has passed along a short path, most of the optical analysis that exists in the literature, which generally deals with long (> 100 m) paths does not really apply. Most work on electromagnetic wave transmission through turbulence started with issues associated

with radar and microwave transmission. In those cases, the wavelengths involved need not have been very small in comparison to the structures causing scattering. Transmission of optical frequencies came onto the scene somewhat later, but historically, in all of those cases, the investigations explored the problems of transmission over long ranges. Therefore, my discussion of much of the present theoretical optical work in this field will be limited because it does not apply.

In the optics world, the theoretical starting point is the Kolmogorov's 2/3 law. [14] It is quite reasonably assumed that within the inertial range, $\eta < r < L$, there are a series of interacting turbulent scales that evolve on a time scale much more slowly than the time it would take light to trasverse them. This is in essence, Taylor's "frozen in" hypothesis as applied to optics. It should also be repeated that the evolution of an eddy in turbulence occurs on a time scale much longer than the time it would take sound to traverse the eddy. This justifies the assumption of incompressibility that went into the earlier discussion of the Navier-Stokes equations.

What makes the scales scatter light in the first place is a fluctuation in index of refraction. This fluctuation in index of refraction occurs because regions of air at different temperature will have different densities and as a result different indices of refraction. The concept is that these regions are carried by the turbulence as a "decoration" and that they will follow a spatial structure function in the same way as the Kolmogorov law. In the literature [14] structure functions (1.41 - 1.43) become expressions for temperature by replacing the constants C and ε with C_T. This is justified by assuming the energy dissipation of the cascade to be constant. Of course, that implies that one could write a constant for index of refraction fluctuations

following the same form as well. In the world of optical turbulence, eqs. (1.41 -1.43) become:

$$D_n(r) = \begin{cases} C_n^2 r^{2/3}, & \eta < r < L \\ C_n^2 \eta^{-4/3} r^2, & r < \eta \end{cases}. \tag{1.56}$$

The constant C_n is squared in eq. (1.56) out of convenience for other optical calculations. C_n^2 is called the index of refraction structure parameter.[14] It is called a constant, and treated as such in the literature, but that is a misnomer. It can vary spatially over a propagation distance as the beam goes through regions with different atmospheric conditions. Since what is measured are optical intensity fluctuations in a beam that has traversed some long range, of unknown air conditions, it is possible to generate the same value of optical structure parameter in infinitely different ways. A long enough range of relatively placid air – which would not be considered turbulent by any fluid definition could easily produce enough scattering and interferences to yield an optical signal that was just as broken up or distorted as the same signal going through a comparatively short range filled with actually turbulent air, in the fluid sense. Over a range of kilometers, or even tens of meters, unknown gusts along the path of transmission all contribute to any distortion of an incoming optical signal. There is simply no hope of inversion from the results of a long optical path to the various fluid motions that caused the distorted wavefronts. To make this idea concrete, once phasors wrap around through 2π or more, there is no hope to figure out a unique way what actually happened from all of the possible ways it could have happened. Ultimately, the structure constant is related back to the local ε of fluid turbulence in different regions that the light traverses, which is not a universal

constant itself. In the optical world, C_n is loosely thought of as a measure of the strength of turbulence. Here, this refers to optical turbulence which is realized in the form of temporal and spatial intensity fluctuations at a receiver. It is reasonable to use the index of refraction fluctuation in this manner. Over a long optical range, it is impossible to start from the fluid turbulence itself and derive a more concrete measure, because different regions of turbulent air that the path traverses could all potentially have different regions of flow with varying Reynolds Numbers. As such, someone in the field (in the literal sense of outside in a field) who is trying to make an optical system work, needs some basic idea of how to characterize the range that is being worked on.

At this point, we should point out that intuitively, the smallest scales of turbulence are the ones likely to scatter light the most. This is not just because they are small compared to the wavelengths in question. One would expect that as the vortices stretch and become thinner as they dissipate their energy to viscosity, that there is a more energy flow going to heat over a smaller area than would be the case at the places in the cascade where a new vortex could be formed. This means that there will be a larger difference in index of refraction compared to still air, and hence stronger scattering. From the results of the current experiment, the scales actually observed correspond to the smallest scales of turbulence for flows of the kind examined. One of the central features of our technique is that it preferentially zeros in on the smallest scales and extracts them directly, while hotwire and other measurements have to infer those scales from the phenomenology and laborious analysis, or in the case of PIV, directly look for them in a very lengthy analysis. To

be discussed in a table in the results section, the scales we get directly, because of this preferential scattering, correspond beautifully to the data of others for the Kolmogorov microscale, obtained by other means.

From eq. (1.56) the next standard step is to take a Fourier transform of the covariance function. This produces what is called the spatial power spectral density, or more simply, the spatial power spectrum, denoted $\Phi_n(\kappa)$. After doing the appropriate integrals, it turns out that in one dimension, eq. (1.56) implies that $\Phi_n(\kappa)$ follows a -5/3 power law, and that in three dimensions we have

$$\Phi_n(\kappa) = 0.033 C_n^2 \kappa^{-11/3} \tag{1.57}$$

The factor of 0.033 is a numerical approximation for all of the factors of π and other constants (from gamma functions) that come out of the integration. Eq. (1.50) is called the Kolmogorov spectrum. There are "competing" spectra in the literature which are extensions of the Kolmogorov spectrum and are widely used. They are the Tartarskii spectrum [14]

$$\Phi_n(\kappa) = 0.033 C_n^2 \kappa^{-11/3} \exp(-\kappa^2 / \kappa_m^2), \quad \kappa > 1/L, \; \kappa_m = 5.92/\eta \tag{1.58}$$

and the Von Karman spectrum [14]

$$\Phi_n(\kappa) = 0.033 C_n^2 \frac{\exp(-\kappa^2 / \kappa_m^2)}{(\kappa^2 + \kappa_0^2)^{11/6}}, \quad 0 < \kappa < \infty, \; \kappa_0 = 1/L \tag{1.59}$$

It should be noted strongly that the exponential terms tacked on to the Kolmogorov spectrum are attached only for mathematical convenience and have no firm basis in physics. In their defense, the equations apply in the inertial range by design. There is also a Hill spectrum, [16] but it will not be reviewed here. To see why we want a spectrum at all, we now switch to scattering proper.

Scattering proper

Since most optical turbulence problems are concerned with transmission through the atmosphere, we start by assuming an incoming monochromatic electromagnetic wave solution to Maxwell's equations, and write

$$n(\mathbf{x}) = (1 + n_1(\mathbf{x})), \;\; n_1(\mathbf{x}) \ll 1 \tag{1.60}$$

where this represents small variations in the index of refraction. Here, $n_1(\mathbf{r})$ is a small, isotropic, homogenous, random, scalar field. It is possible to account for variations in index of refraction that have time dependence. However, such variations in real fluids, compared to the transit time of light, render them negligible. Andrews and Phillips give an expression for the magnitude of these variations in index of refraction. [14]

$$n(R) = 1 + 77.6x10^{-6}(1 + 7.52x10^{-3}\lambda^{-2})\frac{P(R)}{T(R)} \tag{1.61}$$

In expression (1.61) units are rolled into the constants such that the index of refraction is dimensionless. We can see that these changes in index of refraction depend on the local variations in temperature and pressure. This is exactly what fluid turbulence will provide. If we were to insert a random field for the index of refraction into Maxwell's equations, and attempt to find wave solutions, the unknown field $\mathbf{E}$ becomes parameterized by the unknown random field $n(\mathbf{x})$, and cannot be solved exactly. Approximation methods must be employed.

The most commonly applied approximation is the Rytov method. It should be mentioned that the Born approximation fell out of vogue when it was observed that predictions calculated with that model did not reproduce observed data.[14,16]

The Rytov approximation seeks solutions to Maxwell's equations of the form [16]

$$U(\mathbf{r},L)=U_0(\mathbf{r},l)\exp[\psi_1(\mathbf{r},l)+\psi_2(\mathbf{r},l)+...] \tag{1.62}$$

where the ψ terms are complex phase arguments. The evaluation of any of the statistical moments of the **E** field when calculated using this expansion (or Born) lead to integrals over $n(\mathbf{r})$ which were Fourier transformed to the spectral density, $\Phi_n(\kappa)$. The spectral density of choice is then inserted into the calculations. Any of the approximation methods, used in the optics literature, like the Born approximation or the Rytov approximation have this feature. Calculating quantities of interest becomes a question of what type of wave (spherical, Gaussian or plane,) what type of approximation, and what spectrum. Much theoretical work in optical turbulence revolves around calculating one of the various combinations of wave type, approximation and spectrum. A comprehensive discussion of all of these combinations is well beyond the scope of this thesis.

The Rytov approximation, and the Born approximation are also limited in application to what is called weak fluctuation theory (intensity variations are not large and multiple null regions are not present in the incoming wavefront). They do not predict the correct statistics for so called strong turbulence i.e. large fluctuations. There is another approximation called the Extended Huygens Fresnel Principle that is

employed for strong fluctuations. Unfortunately, as of this writing, strong fluctuation theory does not seem to fit well with available data.[14,18]

Fortunately, for this experiment, the optical wavelength used, 632 nm is approximately four orders of magnitude smaller than the smallest observed scales of turbulence, in flows like those examined here, which are on the order of tenths of millimeters. Because of this, complicated scattering calculations can be essentially replaced with ray optics.

The air is a linear, nonconducting, nonmagnetic material. We can also assume that the index of refraction varies very little over the wavelength of an incoming ray of light. In the optical regime, we are able to seek solutions to Maxwell's equations that satisfy:

$$\left[\nabla^2 + \frac{\omega^2}{c^2} n^2(\mathbf{x})\right]\psi = 0 \tag{1.63}$$

This simplification follows from the assumption that $n(\mathbf{r})$ varies slowly, since that would imply that the permittivity of the medium varies slowly (compared to wavelength). Therefore, gradients of the permittivity would drop out when they are accounted for in Maxwell's equations. Not surprisingly, this discussion leads to the eikonal approximation.

Following Jackson [17], in the case at hand, solutions ψ, to (1.63) have a local wave number

$$\left|k(\mathbf{x})\right| = \omega n(\mathbf{x}) / c \tag{1.64}$$

and we seek them of the form:

$$\psi = e^{i\omega S(\mathbf{x})/c}. \tag{1.65}$$

The scalar function $S(\mathbf{x})$ is called the eikonal. Equation (1.65) implies that the solutions ψ are plane waves with wave vector

$$\mathbf{k}(\mathbf{x}) = \omega \nabla S(\mathbf{x}) / c = n(\mathbf{x}) \omega \hat{\mathbf{k}}(\mathbf{x}) / c \tag{1.66}$$

What is important to take conceptually from (1.66) is that $\hat{\mathbf{k}}$ is a unit vector that points in the instantaneous direction of $\nabla S(\mathbf{x})$. This is at the heart of the geometric interpretation of the discussion. We make the connection that

$$\nabla S(\mathbf{x}) = n(\mathbf{x}) \hat{\mathbf{k}}(\mathbf{x}). \tag{1.67}$$

Very quickly, this evolves into a problem of variational calculus. When we substitute (1.65) into (1.63) and create an equation for $S(\mathbf{x})$, we are able to neglect the higher order terms because of the slow spatial variation of $n(\mathbf{x})$ compared to the wavelength of the light in question. We can make the eikonal approximation

$$\nabla S \cdot \nabla S = n^2(\mathbf{x}). \tag{1.68}$$

Using this to simplify the math, a Taylor series expansion of *S* becomes essentially a propagator when inserted into (1.65). If we imagine some origin relative to which our plane wave incrementally advances at a position **r**, we invite the geometric interpretation directly by tracing out the ray path *s*, associated with the wave. Specifically, $\frac{d\mathbf{r}}{ds} = \hat{\mathbf{k}}$, $\frac{d}{ds} = \hat{\mathbf{k}} \cdot \nabla$ and $\frac{dS}{ds} = n(\mathbf{r})$. Putting all of this together, we come to the ray equation, or the generalized Snell's law.

$$\frac{d}{ds}\left[n(\mathbf{r}) \frac{d\mathbf{r}}{ds} \right] = \nabla n(\mathbf{r}) \tag{1.69}$$

The above analysis applies to the scattering of light off of one scattering vortex. One could model the vortices as essentially small cylinders or ellipsoids of

random orientation, and attempt to calculate ray trajectories in a computer simulation. However, in terms of the optical analysis of the experiment that was performed, our analysis is simplified even further.

Whatever light came in from the collimated and expanded beam of the laser hit an eddy and even though it was still very strongly forward scattered, we assume that it scattered away from the pinhole of the detectors without interfering with light scattered by other regions of the fluid outside of the narrow cylinder defined by the optical axis and the pinhole. A highball estimate of how forward scattered light from these eddies are can be made by imagining diffraction from a hole or a slit. Using $\sin\theta = \lambda / d$ where d is a correlation length, which we believe corresponds to the Kolmogorov microscale, gives theta ~ 0.0015 rad. The idea is that the pinhole defines a narrow cylinder along the beam axis. Only single scattering from a vortex that lies within this cylinder can affect the amount of light that reaches the detector behind the pinhole. What matters here is that light from another parallel pinhole diameter cylinder will not interfere with the light coming to the detectors if we measure close enough to the interaction region.

In this sense, we are also in a "single scattering regime." Light is very unlikely to scatter away from the detector, leave a viewing cylinder, and then scatter off of another turbulent structure in another cylinder only to enter the detector. The scattering region is optically thin compared to the extreme forward scattering. Specifically, with a forward scattering angle ~ 0.0015 rad, and an interaction region only 30 cm wide, even the small fraction of power diffracted at close to that angle, would not leave the viewing cylinder with a diameter of 0.5mm, to hit another

structure outside of that cylinder before leaving the interaction region. If there was a wide interaction region or a long optical path (the conditions of almost every optical turbulence experiment in the literature) multiply scattered light (in the sense that the light scattered away from the detector, hit another eddy and came back in, or interfered with light from eddies outside the field of view) would certainly reach the detector and that would have to affect the data. We would expect that by going further back, scattered light from a region outside of the pinhole would interfere with the signal coming in from directly in front of the pinhole.

This was checked by taking measurements of correlation length of the same flow, with the detectors at ½, 1 and 2 m distant from the interaction region. There was no appreciable difference in results. Specifically, correlation lengths did not change. Had there been a meaningful contribution to the signal coming in from sources outside the viewing cylinder, there would certainly have been an effect. One of the features of this method of optical measurement of turbulent scales is that it takes much of the more complicated optics out of the analysis.

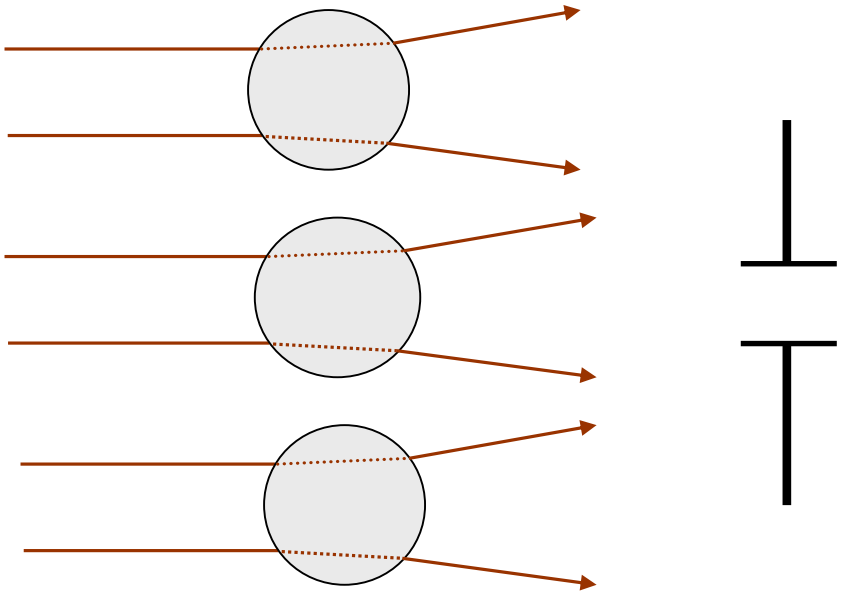

Fig[1.6] The detector apertures in the experiment are close enough to the source of scattering, and the scattering is so forward that any scattered light coming in from a source outside of the cylinder of view defined by the aperture will not enter the aperture. This greatly simplifies any discussion of the optics.

Chapter 2: Experimental procedure

Overview of the Experiment

Equation Chapter 2 Section 1

In brief, the experiment examined correlation lengths and times of sections of an illuminated column of laser light in real time. This was done by expanding a 10 mW HeNe laser beam with a focused 30 mm beam expander and shining the light through a region of turbulent air. The turbulence was freely decaying grid turbulence generated by an industrial strength blower. The turbulence was blown at a right angle to the beam path and the portion of the flow, that the beam traversed, was approximately 30 cm wide, with its edge approximately 20 cm from the beam expander. The mouth of the blower was 60 cm from the beam axis for most measurements, though comparisons were made to a 30 cm displacement for one measurement. A hot plate was placed directly in front of and underneath the output of the blower which could be set to different temperatures and thus provide more intense scattering centers to be picked up by the flow. On the other end of the range, 1 meter from the beam expander, the column of light was split and sent to two silicon photo detectors, which were both fitted with pinholes and optical filters. The difference in optical path length between the two detectors was 30 cm. The detectors were mounted such that they could be displaced either vertically or horizontally relative to a

common zero in the center of the incoming disk of light. The signals from the detectors were converted to digital signals by a DAQ and then sent into a computer for analysis. The computer could then be used to construct both time and spatial correlations in real time. From this, the time scales and spatial scales of correlated shadows of the fluid turbulence could be determined.

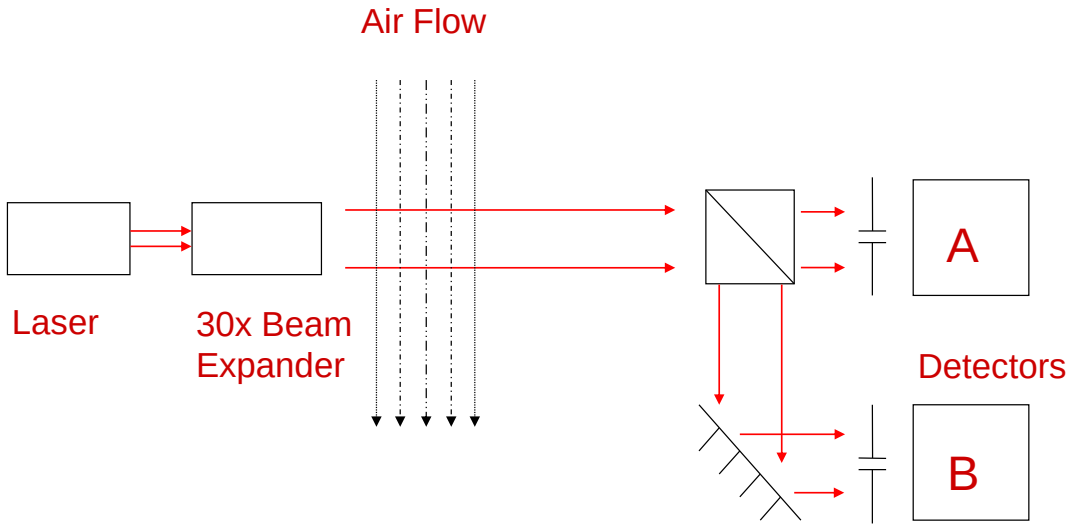

Fig[2.1] Experiment schematic. The expanded beam formed a disk in the plane perpendicular to the apertures on the detectors. The detectors could be translated to look at different regions of the disk. The mouth of the blower was in general 60 cm from the beam axis.

The genesis of the experiment was to probe what happens to light as it passes through a turbulent medium by examining correlation length and time scales and thus gain insight into the breaking up of wave fronts in strong optical turbulence. Again, the core mechanism is that pockets of air at different temperatures create scattering centers and the more scattering the more the signal would be affected. It turned out that the technique was not particularly useful for long range experiments, in the far field, over the range of a typical optical link. This is because there are an infinite number of ways for scattering phenomena to propagate into the far field to produce

the same results. Once multiple scatterings lead to light entering the detectors, one could produce a short correlation length optically with relatively placid conditions, but with a long enough range, while one could produce the same short scale results by having extremely turbulent air (in the fluid sense) over a shorter range. There are many other confounding factors. Lensing effects of larger hot pockets of air could shift the entire beam away from the detectors, rendering a run very difficult to perform. A strong gust of air in the middle of a long range might not be noticeably different from two gusts of air at different places in the range, and there was no way to measure conditions at regular intervals over the long range. Most importantly, if one wanted to examine a nicely turbulent pattern of received light intensity, the wind would not cooperate by maintaining steady conditions relative to the time it took to take a statistically meaningful measurement. Over long distances, there are simply too many confounding factors and too many unknowns about the conditions of the air through which the beam travels as it goes down the range. In this situation it is difficult to obtain meaningful results beyond qualititative observations that the beam was getting more randomized in the given weather conditions and range, over a short period of time relative to various different and unknown weather conditions, such as varying wind gusts.

However, in the near field, single scattering regime, under controlled circumstances, our experimental technique provides robust and highly precise measurements of small scale turbulent structures. The theoretically accepted picture of many scales of turbulence composed of stretching and twisting vorticity structures,

that concentrate at the smallest scales, led organically to the idea of using optical techniques involving correlations to probe these structures.

In a laboratory environment, at close ranges of less than a meter, flows of a consistent nature could not only be reliably reproduced, but could be examined without the problems associated with either multiple scatterings or multiple unknown and uncontrolled sources of turbulence. Reproducible flows could be produced and maintained over multiple runs. The environment was temperature controlled and humidity controlled.

If the two detectors were close enough to the scattering region, scattered light from regions other than those the detector was looking at directly could not enter the detectors. It was found by direct measurement that varying the path length from the center of the turbulent region to the beam splitter and hence the detectors, from 50 cm to 2 meters made no discernable difference in correlation lengths. Measurements were made at 0.5m, 1m and 2m to verify this.

Temperatures could be held constant. Background light could be essentially eliminated, though with the filters as tight as they were that was not as much of a concern indoors. We could directly, and reproducibly, probe the shadows of structures in turbulent flows passing transverse to the beam line. Those shadows corresponded to a slug of turbulent air passing in front of the detectors, and because of the complicated structure of that slug, one could tell when it had passed because the two detectors would no longer correlate. What had started as a project that examined long range links became a probe into the structures of fluid turbulence itself.

The length scales measured by this examination corresponded to the smallest scales in the turbulence because of the structure of turbulence itself and the nature of the measurement. As was discussed previously, most of the structure of a turbulent flow is of the smallest scales, and because in our experiments, for the light reaching the apertures of the two detectors to correlate, these apertures cannot be much further separated than that small scale.

To justify that assertion, consider the following picture. Imagine a pile of thin sticks of the same length lying on the ground. Light is shining up through those sticks. The light makes a complex shadow pattern when it passes through. The largest size scale of that shadow pattern that can result is, of necessity, the length of those sticks.

Now imagine two detectors, of an aperture diameter close to the scale of those sticks looking down on those sticks. Both detectors can agree by correlating their signals whether the extent of a shadow pattern that both are looking at is the same shadow pattern. The scale over which they can do this is the scale of the sticks. If you move one detector away from the zero position, in any direction, where both detectors started from looking at the same place, by two stick lengths you are guaranteed to be looking at a completely different shadow configuration. If you imagine that the diameters of the apertures exactly match the stick lengths, then a "one stick" displacement could still have half of the same stick in one detector and the other half in the other, and there would still be a correlation. However, by two stick lengths it is impossible for that same stick to seen by both detectors. We can thus conclude, that provided the apertures are on the scale of the stick lengths or

smaller, and the 0.5mm apertures were for the flows examined, that the correlation lengths measured must correspond to the scales of the sticks in the pile.

In the case of turbulence and the actual experiment, those sticks are of course, the actual fine structures in the flow itself. The laser light is scattered by those fine structures the most. The small structures concentrate heat, therefore they scatter more. Another argument for why the detectors focus on the small scales of turbulence is that a comparatively large blob of air that contains the smaller ones is going to scatter light in the same way across its entire dimension and create a sort of constant background – on top of which the much higher scattering small structures are overlaid and because the experiment measures a demeaned fluctuation, a more slowly changing background will contribute less to the correlation.

The chaotic nature of turbulence guarantees that the actual configuration of filaments and eddies in one slug of air will be completely different than the configuration in the slug of air next to it. The two slugs will make completely different shadows. There will therefore be no "fooling" of the correlation by some sort of unexpected repeating condition. Once the detectors are looking at patches of air that are separated by much more than the length of the structures, they must be looking at an entirely different shadow configuration, and will no longer correlate. Since those length scales are dominated by the smallest scales of turbulence, we can be confident that we really are looking at the small scale structures of turbulence.

This is one of the reasons that later measurements were switched to vertical displacements only. The presence of the mean flow itself could affect the results. For a spatial correlation measurement, shifting horizontally meant that there would be

some portion of the correlation contributed to falsely by the patch of air seen at detector A having the time to blow downstream in front of detector B a moment later and thus make the length scale seem slightly longer than it actually was. By displacing vertically, the patch of air being sampled was blown out of the field of view of both detectors at the same time. Since the fully developed turbulence is isotropic, this was completely justified.

Details of the Experiment

For this experiment, four sets of apertures, of four different diameters were machined. The apertures were 2mm, 1.5mm, 1mm, and 0.5mm respectively. The 1.5 mm apertures were never used. Steps of half an aperture width were taken to be the standard displacement in any experimental run. Since at first, we did not know what sorts of scales we would find when we looked but, knew they had to be on the scale of a millimeter, we simply started with the 2 mm apertures and worked our way down until we had found a sufficient resolution to see a smooth spatial correlation. The 0.5 mm apertures turned out to work quite well at resolving the spatial correlation sufficiently to make reliable measures of the scales that were being observed.

Doing the experiment with even smaller apertures would have added more resolution and perhaps made the measured length scales even more precise, however, that was not possible given the physical limitations of the equipment available. In order for this experiment to work, setting a good zero position was essential. The zero position was defined as the position where both detectors were looking at the

same slug of air at the same time. This meant aligning them so that their fields of view overlapped each other as much as possible.

This was accomplished by placing a pinhole in front of the beam splitter. This produced two laser dots, which were physically on the order of 1 mm diameter, respectively on the two pinhole faces of the aperture. When aligning apertures that were larger than 0.5mm, a larger initial pinhole was used, however the procedure was unchanged.

The first dot, transmitted to the face of the aperture A was aligned so that the pinhole of A appeared in the center of the laser dot. Once that was set, it was not touched. Aperture A did not need to be in the exact center of the dot, it was however useful to use the center as a visual cue for the first order of the alignment. The mirror that directed the beam to aperture B was then adjusted to align that dot so it would be centered on the pinhole of aperture B.

This was only the first step, however. The correlation itself was used to guide the fine adjustments. Since the device could calculate correlation functions very accurately in real time, and since the correlation function was giving significant figures out to 4 decimal places, the fine adjustments were made by attempting to get correlations as close to one, for the auto correlation bin, as much as possible. If the two detectors weren't looking at the same thing, they simply would not correlate. In this sense, the system "aligns itself." The procedure then was to make fine adjustments on the mirror and watch the effect of moving in that direction on the autocorrelation. For a given run, using the smallest apertures, 0.5 mm, victory was

usually declared when the autocorrelation was above 0.975. But for many runs, the starting autocorrelation was better.

Alignment could be more of an art than a science. If realignment was required because the He-Ne laser had been disturbed or if the system was displaced to take data downstream, sometimes a greater than .99 autocorrelation would occur within a few minutes of work. Other times, it could take a quarter hour. However, once the routine became practiced, it could generally be finished in less than five minutes. For obvious reasons, it is much easier to align larger apertures than smaller ones by this method. The larger the aperture was, the less a small deviation in alignment would change the total viewing area the detectors overlapped. When the centers of the pinholes were close to each other, there was more common light.

This also put one of the physical limitations on the experiment itself and is one important reason that apertures smaller than 0.5 mm were never used. The apertures were cut out of copper, made as flat as possible and then covered in flat black paint. The paint had a slight variation in its surface, no matter how carefully the disks were machined and painted. Telling the difference between the opening of an aperture of say 0.1 mm (the smallest drill bit available) from a dark point in the laser speckle pattern was not something that could be done with the naked eye for the first alignment. There are many ways that this difficulty could be overcome in a more refined version of the device, however, since the 0.5 mm openings were already giving adequate resolution for the flows under study, such changes that would have been expensive and labor intensive were not pursued. One obvious solution would have been to precision manufacture apertures out of a very smooth material that was

already black and (critically) would allow the drilling of very narrow clean holes. This is why just finding some black plastic was not the answer. Then one could have used a magnifying glass to look more closely at the first alignment. However, fine alignment using the mirror would then become much more difficult to do by hand because of the increased sensitivity to misalignment. One could imagine a dream version of this device that would have the fine mirror adjustments done mechanically while a computer used a routine to maximize the autocorrelation.

The main reason that apertures smaller than 0.5 mm were not used to gain even higher resolution of the spatial correlation function was the amount of transmitted light. As it was, with a 10 mw laser and the detectors used, which had seven stages of gain, the maximum gain settings needed to be employed in order to insure a high signal to noise ratio. We wanted at least one volt base output coming from the detectors into the DAQ. Base inputs to the DAQ were on the order of 1 - 1.5V for 0.5mm apertures. With 0.5mm apertures, voltage fluctuations (the signal) were on the order of 0.02V with the detectors set to maximum gain.

The DAQ was advertised as 16 bit, however, the last three bits of the data were noisy. This was directly measured by observing the output of the DAQ with a terminator installed on its inputs. It seems that many DAQs have a feature like this and advertise that they are 16 bit based on taking averages. As it is, 2^{13} "guaranteed" distinct steps translates into 8192 steps. This produced the fundamental limit of 4 significant figures of the signals that were then processed by the computer.

To improve the device and gain even higher spatial resolution, by machining and installing smaller apertures, there are three obvious options. Employ a brighter

laser. Employ a better DAQ. Employ more sensitive detectors to place behind the pinholes. All of these things are quite easily accomplished.

Of all the equipment used in this experiment, the most crucial was the data acquisition system (DAQ). The DAQ used in this experiment, was a 9215-A DAQ from National Instruments. It is a 4 channel standalone unit that can communicate directly to a computer via a USB port. It samples at 100kHz per channel and was chosen because it specified 16 bit resolution, is easily portable and readily communicates with multiple platforms by virtue of the USB connection. It has the advantage of being designed specifically to operate in the Labview software environment. While the device still needed to be configured with the Labview software, using the National Instruments device explorer package, the device was essentially plug and play and it was easily possible to set the scale of incoming signals and sampling rate from within the Labview code itself. Unfortunately, the DAQ had three noisy bits and only 13 were really useful. This was directly measured by examining the output of the DAQ when its inputs were terminated. This three bit error was a limiting source of error in the experiment.

The photo-detectors themselves were Thorlabs PDA36A silicon detectors. They were rigidly mounted with their faces perpendicular to the beam axis. These detectors have a 17MHz bandwidth, a wavelength acceptance range of 350-1000 nm, a 13 mm^2 (3.6mm x 3.6mm) active area and a gain of 1.5×10^3 V/A to 4.75×10^6 V/A. Since our experiment did not sample faster than 100kHz, there was more than sufficient bandwidth. The switchable gain had eight steps up through 70dB, and it was generally desirable to use the highest gain setting in order maximize signal to

noise with the smallest apertures. This gave outputs in the region of 1-1.5 V. With a larger aperture, it was easy to saturate the detectors on high gain. The detectors were very quiet even on maximum gain. Excluding 60 Hz noise, which was removed immediately by sampling at a much higher rate than 60 Hz, and demeaning, the noise from the noisy three bits of the DAQ provided a much greater contribution. The responsivity of these detectors peaked at close to 700 nm making them very suitable for use with a He-Ne laser.

The detectors are manufactured in such a way that they can be fitted with a filter that screws into a cylindrical mounting directly in front of the active region. Narrow band filters were mounted and the housing for them was approximately 1.5cm long and 2.7 cm in diameter. The pinhole apertures were affixed to the lip of the housing using wax. In this way they could be quickly swapped out and mounted. Since the wavelength of the light used is very small compared to the aperture opening, there was little to worry about from diffraction effects. The active region of the detector was large enough to catch all the light that was transmitted and since we were only measuring intensity, diffraction was of no concern. If one were to use a much smaller aperture in this sort of experiment, provided that there was enough light, sensitivity of the detector, and resolution from the DAQ, diffraction effects at the pinhole would still be of no concern.

The detectors were fitted with Thorlabs FL632.8-1 laser line filters that have a peak at 632.8 nm and a FWHM of 1 nm. They came pre-machined to mount on the detectors. They are 25.4 mm in diameter and 6.3 mm thick. These filters were designed to be used with a He-Ne laser and they cut down tremendously on any

background noise or optical contamination from other sources. The filters were absolutely necessary. Without them, the instrument could easily pick up the oscillations of laboratory ambient lighting. When taking data indoors the extra precaution of working in the dark was taken.

The pinhole apertures were machined by hand. They were pressed out of stiff copper sheet by a die to a diameter of 3cm and pressed flat. They were centered and drilled to the requisite diameter. Centering of the pinhole was done as carefully as possible, but exact centering was not necessary because of the comparatively large active region of the detector a short distance behind them. The apertures were pressed again a second time to insure they were flat and given two coats of flat black paint to prevent any unwanted reflections. It is possible that the process of painting made the diameters of the pinholes slightly smaller than reported. However, if they were very slightly smaller than reported, this is a small error in favor of the correlation measurements being more accurate because a smaller pinhole only means a higher resolution in determining the correlation function.

The detectors were mounted on optical translation mounts that could be adjusted both vertically and horizontally by micrometers. The accuracy of the translations was +/- 0.005 mm. In the experiment, a vertical translation is one that occurs in the vertical plane perpendicular to the beam line and horizontal translations are parallel with the flow. With this arrangement it was possible to translate the detectors to a full 28 mm separation if both detectors were moved. However, when taking data indoors, it was never necessary to go out further than 5 mm, because in

general, the signals had become completely uncorrelated by the time the detectors were separated by 4 mm.

The beam splitting cube was 4 cm on a side and polarizing. It was offset by a small angle to insure that there would be no difficulties with retro-reflections. Great care was taken to make certain that the polarized laser was rotated such that both detectors were reading the same average voltage as closely as possible – usually to within 0.1V. This was accomplished by making a small rotational adjustment and reading the two outputs. The process of demeaning insured that good data could still be obtained even if the average voltage from one channel was significantly larger than the average voltage of the other channel. However, this alignment insured that the signal to noise ratio from both channels was comparable. The bottom of the cube was held in place with wax and fitted to a machined aluminum base that screwed down into an optical breadboard. This ensured that the cube would be of the proper height to fully interact with the beam region.

The beam expander was a 30x beam expander purchased from Melles Griot. In the course of examining the beam expander, it was discovered that in two small circular patches, the primary lens coating was not even, and this caused a significant drop in intensity transmitted though those regions. Fortunately, those two patches fell on roughly the same diameter as the main lens. Measurements were taken of the intensity across paths that did not have those occlusions by simply rotating the beam expander. The beam profile along those lines (both horizontal and vertical) was nicely Gaussian and smooth. The occlusions were also more than 5mm from the center of the beam. Since that was more than the decorrelation length of any

measurement made indoors, this was not an issue. It should also be noted that by keeping one pinhole fixed and displacing the other by up to 5mm, we were still in the region of the expanded beam that could be approximated by a plane wave.

The DAQ used was a 9215-A DAQ from National Instruments. It is a 4 channel BNC connecting standalone unit that can communicate to a computer directly by USB port. It samples at 100kHz per channel and was chosen because it advertizes 16 bit resolution, is easily portable and easily communicates with multiple platforms by virtue of the USB connection. It also has the advantage of being designed specifically to communicate with the Labview software package. While the deivce still needs to be configured in the Labview software, using the National instruments device explorer package, this makes the device essentially plug and play. This ease of use was of great benefit because it was possible easily set the scale of incoming signals and sampling rate from within the Labview code itself.

The computer code

One of the largest selling points of this technique to probe turbulent scales is that it can be done on the fly. What made this possible was the code that was written to do this.

The code was written in Labview which was chosen because it specifically supports the DAQ that was used. Both are National Instruments products. Labview is an object oriented language that uses graphical components which represent blocks of computer code as building blocks. Programming in Labview consists of choosing operations from many pallets and then connecting them in a way that is reminiscent

of plumbing or circuit boards. For example one selection from a pallet might be a box that represents telling the computer to take data in from the DAQ. From there, the data is graphically represented as traveling in pipes to other blocks of code that will manipulate it in some way. At the outset, it is a very friendly and intuitive language to create code in and it is very powerful. However, like all code, there are tricks of the trade and some very non intuitive steps that sometimes need to be taken to make it behave as desired. The code is printed out in the appendix.

The code needed to do three things. It needed to calculate

$$B(d) = \left\langle \frac{\Delta I_A(d)\Delta I_B(0)}{\sigma_A \sigma_B} \right\rangle$$

for both time and space displacements. It needed to do the calculations in as stripped down and efficient a way as possible, so as to not choke the processing speed of a computer running Labview. Finally, it needed to be able to save the collected data and calculations.

The core algorithm of the code is iterative and given by:

$$I_{n+1} = I_{n-1} + \left(I_n - I_{n-1}\right) / N$$

which is a running average that was calculated on the fly for both channels and then fed into the subroutines that calculated deviations. This is the same algorithm that is used in digital multimeters and allowed for a dynamic mean to be taken. As can be seen, the effect of this is to create a sliding window that corresponds to each new data point being averaged with the average value of the last N averages taken in a cycle that repeats until stopped.

The algorithm that determines the correlations must use an appropriate dynamic mean of the local (temporal) intensity by subtracting a local running average intensity from each incoming reading. This was a crucial step. For short paths in turbulence, the intensity variations are a very small effect. They are not visible to the naked eye. The dynamically corrected correlation was used both to increase sensitivity and to remove the effect of a non-constant laser output. Laser output varied over minute time scales and collecting a running average over three minutes or more would produce a false correlation without this step. Other noise could also easily effect this sensitive measurement. Therefore, it was necessary to examine fluctuations from a local mean rather than a global mean. Finally, the many different scales in fluid turbulence itself meant that our averaging had to be able to detect the small local variations in the flow with respect to time. Thus, any statistics based on a global mean would be meaningless.

Unless explicitly stated otherwise, the algorithm used an initial average of the first 1000 readings, for each channel, as a starting point I_0. This was done for each channel respectively. For these measurements N = 1000. Sampling was carried out at 100 kHz, meaning that the local average window was 0.01 seconds long. This local mean was used in all of the subsequent calculations of the correlation algorithm. The code was written so that both N and the number of points in the initial average could be varied. It was found in practice that varying the initial average for I_0 made very little difference. An initial average with as many as 1,000,000 points produced results indistinguishable from runs using 1000 points. The window size needed to be large enough to have a meaningful average to de-mean an incoming reading, but the

time that was needed to take that average still needed to be substantially less than any laser variations – which could be accomplished by .01 seconds easily. This is how 1000 samples were decided on as the window size. In practice, for spatial correlation measurements even taking a 1000 sample window at 10 kHz, or even 5 kHz, producing an order of magnitude difference in the time represented by taking that average, there was no measurable effect. However, in order to resolve the time correlation function, it was necessary to sample at 100 kHz. Taking a smaller window than 1000 samples, even down to only 50 samples also had no detectable effect because of the large number of demeaned points averaged over in a typical run.

Great care was taken to strip down and optimize the code as much as possible in order to insure that there was enough computing power to guarantee that running the code at a high sampling rate would not cause the computer to miss data points. The overall Labview program has diagnostic tools installed to allow one to see how much time a given cycle of the code takes from the computer. There are also tools to shut down unneeded processes from sources other than Labview in order to free up computing power when running Labview. For the computer that was used indoors, 100kHz sampling rates were easily obtainable. For the laptop that was used outdoors, it was not possible to sample at a rate greater than 20kHz. In any case, 100kHz was also the maximum possible sampling rate of the National Instruments 9215-A DAQ that was used.

Hotwire Annenometry

In order to create a point of comparison with other experimental techniques and to compare with the existing literature, measurements were also made with a hotwire anemometer. Special thanks must be extended to Professor James Wallace of the University of Maryland for lending both his equipment and expertise to this endeavor. His excellent book on the topic was also of very great use.

Hotwire anemometers work on the principle that a heated thin wire will cool as air blows over it via forced convection, and that the resulting change in resistance of the wire, can be measured and directly related to the velocity of the flow that caused the cooling. The wires commonly used for such an application vary in length from .15 mm to 1.5 mm. In general, their diameters vary from 0.5 μm to .5 μm. [23]. The wire of a hotwire probe is mounted on a small two pronged fork and is usually mounted such that the wire is perpendicular to the direction of the average flow.

For small changes in temperature, it is legitimate to use a linear approximation for the relation between temperature and voltage

$$R_s = R_f \left[1 + \alpha (T_s - T_f)\right] \tag{2.1}$$

where *R* Is resistance and *T* is temperature. The subscripts *s* and *f* refer to sensor and fluid respectively and α is a constant of proportionality which is dependent on the type of wire and measured in reciprocal degrees. Bernard and Wallace report that α is approximately 0.004 K^{-1} for tungsten and platinum wires. In our experiment, $R_f = 3.26\,\Omega$ and $\alpha = 0.0036$.

The next step is to develop a relationship between convection and wind speed.

In general, the thermal energy balance of a hotwire probe is modeled by a simple differential equation.

$$\frac{dQ}{dt} = P - F \tag{2.2}$$

where $P = I^2R = IV$ and F represents the total rate of heat transferred to the fluid. V is the voltage drop across the hot wire.

From (2.2) it can be quickly inferred that hotwire probes can be run in either a constant current mode or a constant voltage mode. In our experiment, a constant voltage probe was used. A constant temperature hotwire circuit is essentially a Wheatstone bridge that is dynamically balanced while the resistance of the hotwire itself changes.

In general F is a complicated function of the Nusselt number, the Prandtl number, the angle of attack of the flow relative to the wire and the physical properties and dimensions of the hotwire probe itself. Fortunately, for a broad range of applications, forced convection and the relationship between temperature changes, output voltages and hence, air speeds can be modeled via King's law.

$$V^2 = A + Bu^n \tag{2.3}$$

Here, V is the voltage drop. *A*, *B* and *n* are constants and *u* is the average local fluid speed. To calibrate the hotwire probe, one must measure the average voltage output from the anemometer for a given flow speed and use a fit of this curve to determine the constants *A*, *B* and *n*. The constant *n* is equal to 0.45 for most laboratory situations.[23]

For our experiment, we employed an AN-1003 hotwire anemometer, which was manufactured by AA Lab Systems. This was the unit which contained all of the electronics. The probe itself was a Dantec Dynamics 9055P0011. Only one probe was used for our hotwire data collection. The time correlation was recorded from that one probe, which was mounted so that rested in the middle of the illuminated region of the flow. The hotwire was perpendicular to the flow. The hotwire signals themselves were transmitted to the same DAQ as used by the optical experiment and processed with the same software on the same computer. This equipment was graciously lent to us by Professor James Wallace.

Chapter 3: Experimental Results

Some Details and Terminology

Before entering into a discussion of the results, some details in labeling need to be pointed out. The overall air speeds associated with labeling a given data set are those measured at the mouth of the blower. This speed was chosen so as to estimate the Reynolds number and categorize the flow. Downstream, the mean velocity of the flow lessens as its kinetic energy is converted to turbulent scales and dissipated to heat. For example, 60 cm from the hotplate, in the stream wise direction, the mean velocity of the flow would be on order of 7 m/s for a flow that left the mouth of the blower at 12 m/s. Similarly, the temperatures reported were those taken over the hotplate, at the level of the mouth of the blower, with the hot plate on and the blower off. The temperature given is recorded as a reference to distinguish different flows. It is not the mean temperature of the flow in the illuminated region. In general, the temperature dropped off very rapidly with distance downstream. For example, on one day's run, the ambient laboratory temperature was $23.6° \pm 0.1°$ C and the temperature in the interaction region, 60 cm away from the mouth of the blower, with the blower pushing air at 12 m/s, was $24.3° \pm 0.1°$ C when the temperature measured at the mouth of the blower was $88°$ C. By the time the flow crossed the interaction region, its mean temperature was essentially room temperature, particularly for flows where the hot plate was not on the maximum setting.

The hotplate, when on, was certainly contributing a disturbance in the air of its own. No attempt has been made to completely model the flows under consideration. However, using the basic phenomenology of turbulence and an estimate for the Reynolds Number based on the flow rate at the blower, and a length scale generated by taking the diameter of a circle to be equal to the area of one of the blower's mesh cells, we can produce the following table as a loose guide to the flows in this experiment.

Re	*u(m/s)*	$\nu(m^2/s)$	η *(mm)*	t_{diff} *(s)*
24,800	*12*	$15.68x10^{-6}$	*1.6*	*0.17*
20,000	*9.7*	$15.68x10^{-6}$	*1.9*	*0.24*
18,000	*8.7*	$15.68x10^{-6}$	*2.1*	*0.28*

Table[3.1] A loose guide to characterize the different flows in the experiment based solely on the phenomenology of turbulence, the air speed at the mouth of the blower and our estimate of Re. $\nu(m^2/s)$ was taken for air at room temperature and one atmosphere. The quantity η is taken from phenomenology, $\eta \sim L\,\mathrm{Re}^{-3/4}$ and will be refined by direct measurement.

In order to orient a discussion of the results, I mean the following things by the following statements. Horizontal displacements are those taken in the streamwise direction. If the stream is in the x direction, this means that one detector is translated parallel to the stream, in the x direction, in the x-y plane. Likewise, vertical displacements are those perpendicular to the flow, in the y direction, in the x-y plane. The expanded beam comes in along the z axis, across the interaction region with the turbulent flow, and its cross section is a circle in the x-y plane.

Time correlation, when used by itself, refers to the time delayed correlation function taken at zero separation between the detectors. Autocorrelation refers to the first point of a time cross-correlation curve for a given separation. Spatial correlation refers to the aggregate of autocorrelations collected at different displacements for the same flow. The value recorded at 1mm on a given space correlation, for example, is the zero (as in zero time delay) of the time cross correlation taken at 1 mm separation between the two detectors. The zero of a spatial correlation function is the time autocorrelation at zero separation, or, the zero of the time cross correlation of the two detectors when they are looking at the same column of light.

A note on errors and error bars

All time correlation curves presented in this work are comprised of one hundred points. Each point corresponded to a time delay equal to one sample cycle. Sampling was in general taken at 100kHz and the correlation algorithm was allowed to integrate for three minutes, unless otherwise noted. This means, in general, that each point represented on such a time correlation curve was generated by evaluating 18,000,000 data points from the incoming signals of the two detectors. This large number of samples, that were evaluated for any given reported point, on a correlation function, gives rise to very high accuracy. Due to this, graphs of time correlation functions will have their error bars suppressed. This is not an attempt to sweep anything under the rug. In general, the average signal coming from a given detector, for a given run, was very close 1V (averaged after 18,000,000 samples). The standard deviation was of order .02V. Using the standard error, then propagating that

error through the correlation function, gives errors bars with scales on the order of 10^{-6}. This error estimate was also confirmed by watching the correlation function integrate in real time over the course of the run and stabilize at five significant figures. However, as noted before, the fifth significant figure was the result of averaging over outputs from a DAQ that only had four completely noiseless significant figures when read by the computer. On a graph, for a single run, compared to a scale of order 1, the error bars would appear simply as lines through the data points. No attempt was made to determine the potential, but certainly much smaller, effect of rounding errors from the processing. As noted in the experimental procedure section, the limiting factor in accuracy was the bit resolution of the DAQ used.

The time correlation itself is an effective measure of the local flow speed. The measured time correlations were very nearly Gaussian. For the 0.5 mm apertures, fitting a Gaussian to one of them and extracting the width consistently produced velocities that were close to the local velocity measured by the hand held anemometer. This is because the time correlation would decorrelate when the slug of air would pass the view of an aperture.

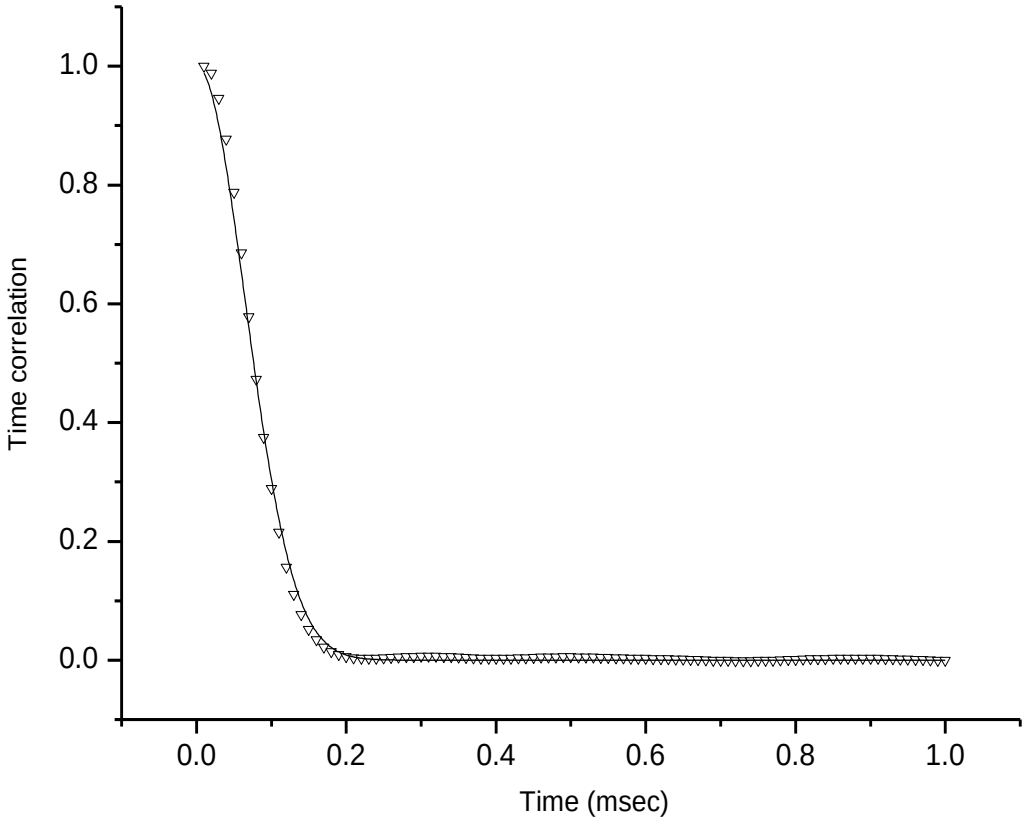

Fig [3.1] A representative time correlation shown with a Gaussian fit. As can be seen, the curve is very nearly Gaussian. In this case, the curve was produced with 0.5mm apertures at zero separation with a Re = 20,000 flow and the beam axis 30 cm from the mouth of the blower. By taking the width of the Gaussian (0.065 msec) and using that to divide width of the aperture (0.5 mm) one obtains a velocity of 7.7 m/s, which agrees with the local mean flow velocity of 7.5 +/- 0.2 m/s as measured by the hand held anemometer.

Time correlations generally had widths of order 0.05ms to 0.1 ms depending on the flow in question. They measured how fast a given pattern would flow past an aperture. A greater mean flow speed meant a shorter width of a fitted Gaussian. The fitted Gaussian widths corresponded to the mean flow speeds when the aperture width was divided by that width.

Spatial correlation functions were constructed by plotting the time cross correlation peaks at different detector separations. The zero of the spatial correlation was the time autocorrelation at zero separation. In other words, successive points in a spatial correlation were the time cross-correlations taken the reported separation distance. One might think this means that for a spatial correlation function, there were more than 1.8 million independent samples taken per three minute run at 100 kHz. Any given run for the spatial correlation would have an error on the order of 10^{-5} for a given point, for one given run as well, if one simply assumed that the error involved would be the same for the time correlation. However, there were larger deviations than that from one run to the next in the recorded value of the spatial correlation function. Those deviations were still quite small overall. This resulted from the constraint that in order to resolve the time correlation, sampling was done at 100kHz. However sampling at that rate insured that over the required time for a light pattern to pass out of view of the detectors, (0.1 - 0.2 msec) the samples would not be completely independent as far as a spatial correlation was concerned. Because of this oversampling, actual errors in the spatial correlation measurements for any given point of the spatial correlation are over an order of magnitude greater than for the time correlation.

Spatial correlation graphs, were produced by averaging these correlations over multiple runs and there were slight deviations in the values of the cross correlations at any given point from one run until the next. In order to compensate for the overlap in sampling, a standard deviation of the averages at one point, taken over 3-20 runs, was constructed for each point, and a standard error calculated. The resulting error bars

were still exceptionally small. However, error bars are visible in those graphs. In general, the errors were small enough that attempting to increase accuracy by taking more runs was considered a matter of extremely diminishing returns.

Once either time or space correlation curves were created, the primary mode of analysis was to fit a Gaussian to the curve and to extract a width. Without imposing a preconception of what sorts of correlation curves should be predicted theoretically, this was deemed an obvious and easily reproducible method to extract meaningful information from the data. The strongest argument that this was a valid method of analysis lies in the strong agreement with the small scales of turbulence as measured by other researchers by other means in similar flows.

Time correlation functions

We begin our main discussion of the results by demonstrating that the transmission pattern of a given small slug of turbulent air is unique. As will be seen below, for the flows studied; length scales were on average, less than one millimeter. By placing 1mm apertures on the detectors, we were not resolving down to the scale of individual small structure eddies. Instead, we were capable of observing an entire pattern of these smallest structures dissipate as it moved down stream with the mean flow, which is shown in figure [3.2]. It should be pointed out that with an evaluation time of three minutes, it is impossible that any correlation at all could have occurred down stream unless the two detectors were looking at the same structures. The plural, "structures" rather than "structure" was used carefully in the last sentence. There are many scales in a turbulent flow, while as discussed; the smallest scales dissipate the

fastest. As the flow moves down stream, we observe the peaks of the correlation diminishing. This is caused by the decay of the smallest structures, and is in general, a feature of freely evolving turbulence. The larger eddies live longer and thus make it further downstream.

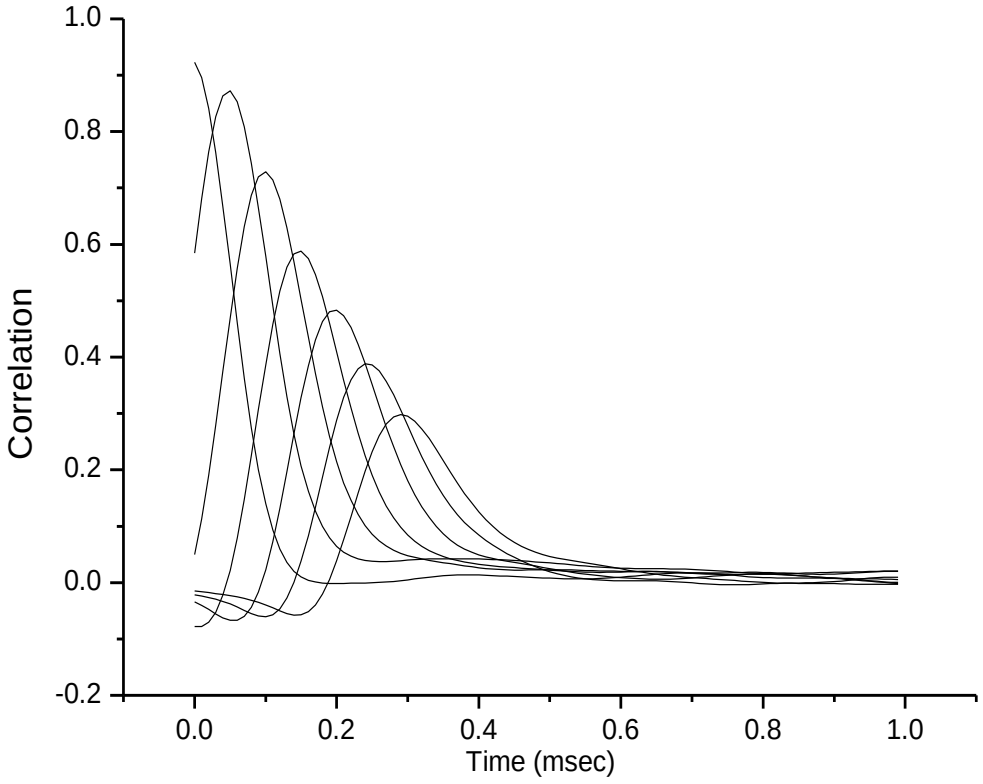

Fig.[3.2] A succession or time correlation curves observed by displacing detectors fitted with 1mm apertures in a stream wise direction at 0.5 mm steps for the same flow. Each curve was generated with a different separation distance between the detectors. The highest peaked curve is the time autocorrelation, where both detectors were looking at the same column of light. Even though this data is represented as smooth curves, in an effort to make a clear image, each "curve" consists of 100 data points corresponding to 100 steps of time delay, and averaged over 3 minutes at 100kHz. Each curve represents a single data run. Error bars are suppressed.

The flow that generated the curves in figure [3.2] was the highest speed (~12 m/s) at the blower mouth with a temperature of 88^{o} C measured at the same point. If we

sample just the peaks of the decaying correlation functions vs. the displacement of the detectors, we find that the subsequent peaks decay in an approximately Gaussian way.

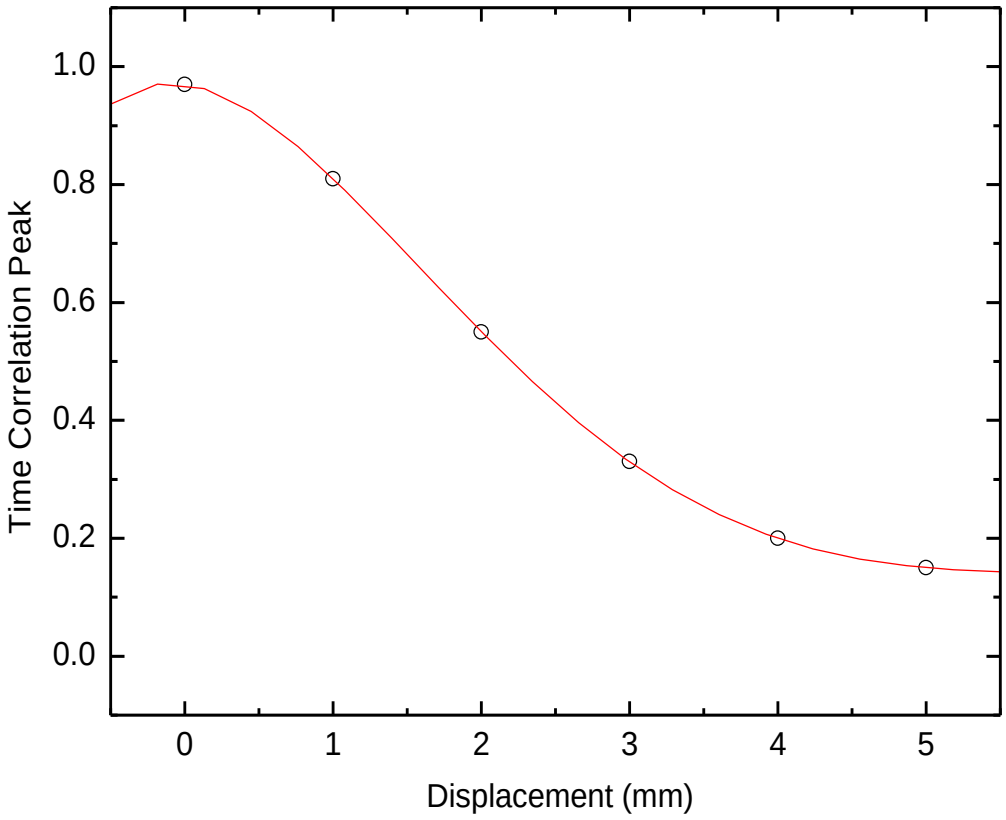

Fig[3.3] The peak of each time correlation function as a function of distance. The detectors were fitted with 1mm apertures and displaced in steps of 1mm parallel to the flow, producing a time lag, as a slug of air moved from one detector to the next. Since the slugs of air are moving downstream with the mean flow, this graph could easily have been labeled in terms of time delay. Error bars are suppressed in this graph because they would be too small to be of use. The data points are shown with a polynomial fit as a guide to the eye only. To extract a width, the first four data points were fit with a Gaussian.

The proof that we really are looking at the same, decaying slug of turbulent air comes from the fact that if one divides the separation distance of the detectors, by the time delay from peak to peak one obtains the local mean flow velocity of 7.14 m/s. The hand held anemometer had measured 7.1 +/- 0.2 m/s for this flow in the interaction region. Fitting a Gaussian to the decay of the first four peaks gives a

width of 2.03 +/- 0.12 mm, which corresponds to a decay time of 0.28 seconds. It should be noted that by simply using the phenomenology of Ch.1, $t_{diff} \sim l_{diff}^2 / \nu = \eta^2 / \nu$, for this flow, with Re~24,800, the eddy turnover time, for those eddies dissipating to viscosity is: 0.17 seconds. This measurement agrees with the phenomenology to within a factor of two.

The peaks above do not fall on a Gaussian. The graph of the peak decay should not be confused with the time correlation measured at a given separation. Actual time correlations did fall on very nearly Gaussian curves – particularly for the autocorrelation. For certain, we are comparing one approximation to another by using a Gaussian fit to discuss a prediction from basic phenomenology. What matters is that these structures can be observed by our experimental technique and that useful information about a given flow can be extracted with that technique. The results that we get are results that should be expected and are easily explained by what is known about how turbulence behaves. A detailed numerical simulation of the turbulence coming off this particular blower, using this particular hotplate, under these particular conditions, would be of little use to anyone – in addition to being impossible to do with the computing power available.

As will be seen below, the small scales that we observed with this apparatus were on the scale of tenths of millimeters. This particular measurement, which employed 1mm apertures to insure entire vortices were included, did not quickly and asymptotically approach zero like a proper Gaussian. Our curve has a tail that is too fat. This is likely due to the fact that the quickest structures to decay will be the smallest scales, while the larger scales will survive longer to go downstream further.

In summary, the time autocorrelation measurements taken with 0.5 mm apertures measured one shadow pattern pass in front of both apertures simultaneously when they were looking at the same region. Those measurements are primarily a reflection of how fast the shadow patterns are blowing by. This measurement of the peak decays taken with 1mm apertures, was following the same slug of air as it evolved and moved downstream. Before continuing, there should be some discussion of how .5mm apertures were settled on for the bulk of the measurements in this work.

Choosing the proper aperture size

The first spatial correlation measurements taken with the apparatus, once it was functional, were with 2.0 mm apertures. While the correlation curve did eventually reach zero, it had a surprisingly gentle slope and it was very clear, that there was insufficient resolution. The initial decay was in a straight line. A pair of 1.0 mm apertures were tried next. Those apertures showed a remarkably faster descent to zero, however the initial decay still was quite linear in appearance. Finally, 0.5 mm apertures were settled on as giving sufficient detail of the correlation to be able to extract a decorrelation width that was physically meaningful. Overlaying the 1mm and 0.5 mm results showed that both had the same essential features. The 0.5 mm apertures produced more of the shape of the actual correlation curve. Sampling with even smaller apertures would surely give more detail, however, the fact that the 1.0mm and 0.5mm zeroed so closely together indicated that the apertures were already on the scale of the structures scattering the most.

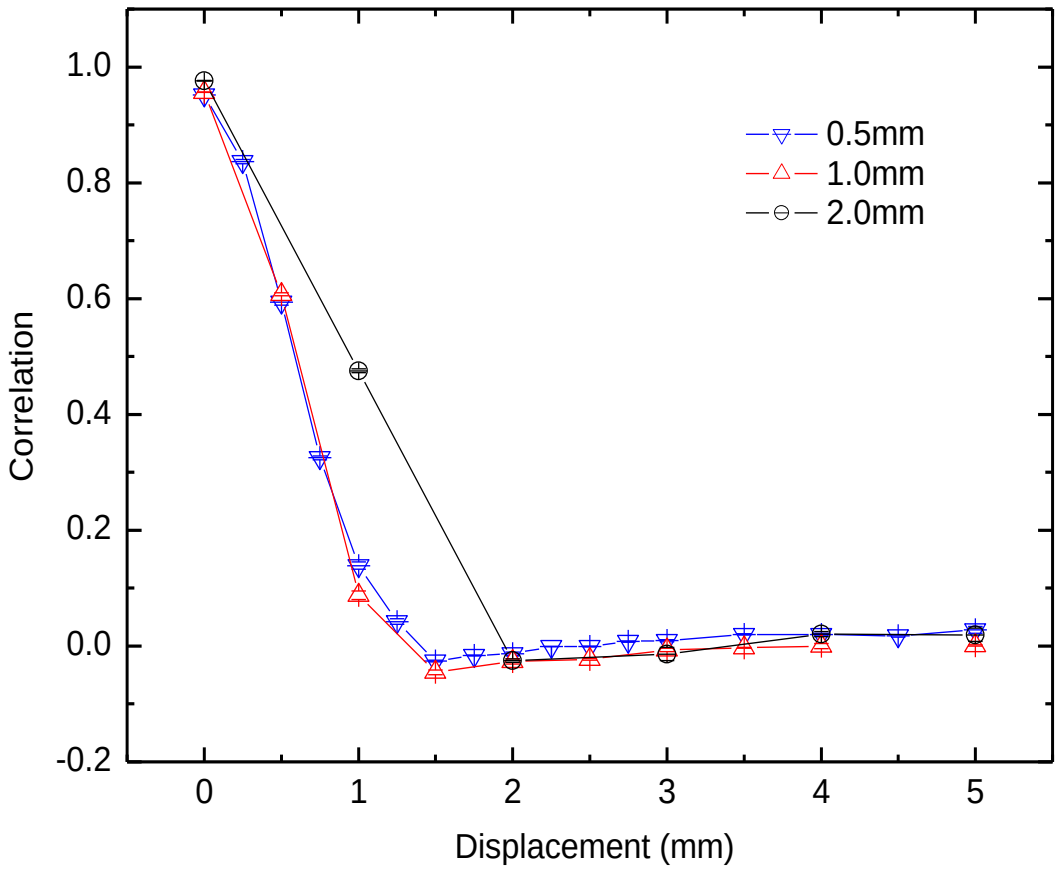

Fig[3.4] The spatial correlation function as measured by different apertures for the same flow. In this case, with a horizontal displacement sampled at 10kHz. With 2.0mm apertures, the details of the correlation function are obscured and the curve takes a misleadingly long time to decorrelate. With 0.5 mm apertures, the details of the curve are sufficiently resolved to make fits and extract widths.

Once it was determined that 0.5mm apertures were sufficient to resolve the spatial correlation function, the next step was to examine different flows.

Spatial Correlations

The first set of experimental runs were done with displacements in the streamwise horizontal direction at a 60 cm displacement of the beam axis from the

mouth of the blower. Most experimental runs were done at this displacement because it was assumed that this distance would give sufficient room for full turbulence to develop. For comparison, later runs were done with the beam axis displaced by 30cm. In the following set of data runs, five types of flow condition were chosen as a way to examine the abilities of the device on a wide range of flow conditions. The blower used had three speeds which correspond to the given Reynolds number approximations. For the measurement labeled "pure convection," an electric hot pad was placed on the optical bench, in front of beam expander in the same area where the flow would normally traverse. This plot represents a flow that is not turbulent. Only gentle convective motions were produced in the air. Nevertheless, they produced a clear signal. The reported temperature was taken at the level of the beam expander. The plot labeled as "still air" represents data with no flow or heating conditions present. This was a sanity check. As expected, with nothing to scatter off of, the light remained correlated across the displacement.

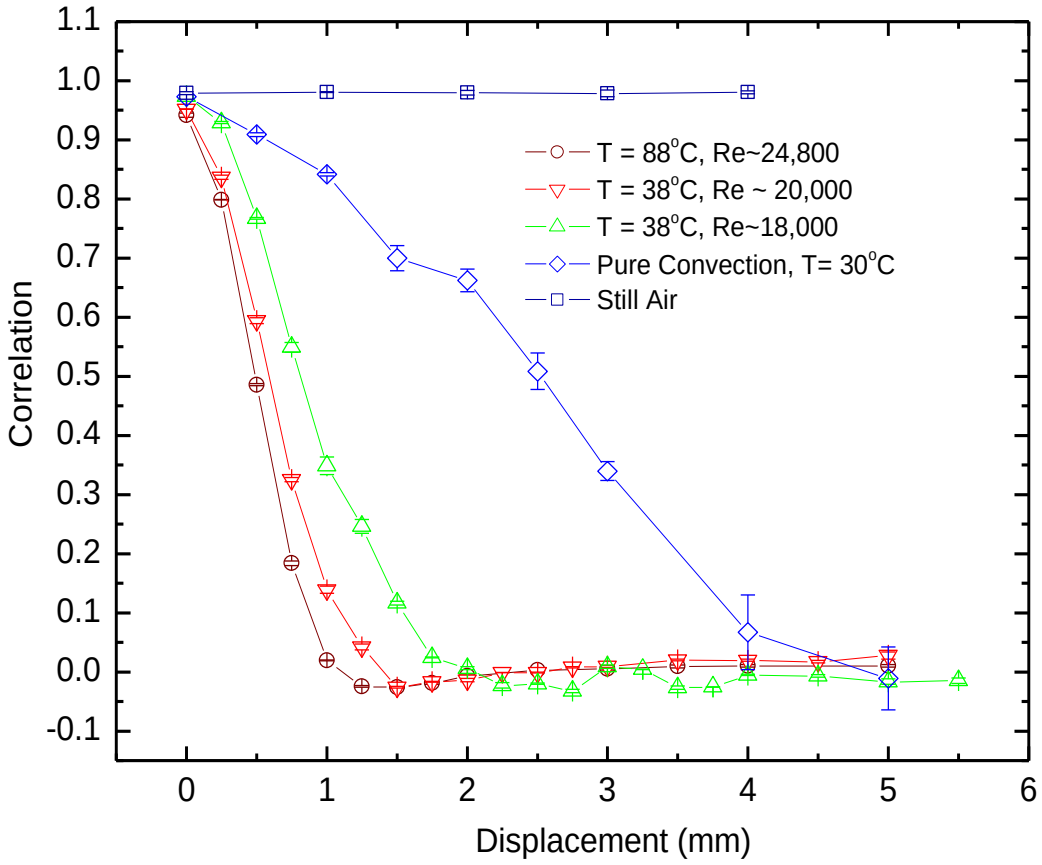

Fig[3.5] The spatial correlation taken with horizontal displacement for different flow conditions with the beam axis 60 cm from the mouth of the blower. The plot of "still air" was taken with no fluid disturbances.

To extract widths from the data, first, the data was normalized to one by division with the peak value of the autocorrelation at zero separation. The data points and the calculated errors associated with each point were fit with a Gaussian to produce a width. We interpret that width as a representation of the typical length scales measured in the flow. A slug of air passing in front of the detector will be comprised of fluid motions on many different scales. Flows with higher *Re* and higher temperatures invariably had only one inflection before crossing zero. However, flows with lower *Re* and lower temperature could have more than one inflection point. For such flows it is possible that two distinct concentrations of small scales are being

observed. All of these measurements were compiled from three runs of three minutes duration at 10 kHz.

The other piece of data commonly extracted was the scintillation. Scintillation is a measure of the strength of intensity fluctuations that were observed during the run. It is the geometric mean of the ratios of the standard deviation of the signal voltage to the mean of the signal voltage, of the two channels. The scintillation is dimensionless and given by $\sqrt{\frac{\sigma_A \sigma_B}{\bar{A}\bar{B}}}$.

	Still Air	Convection	u = 8.7 *m/s* T = 38 *C*	u = 10 *m/s* T = 38 *C*	u = 12 *m/s* T = 88 *C*
Re	N/A	N/A	~ 18,000	~ 20,000	~ 24,800
Gaussian Width	N/A	2.06 *mm* +/- 0.074	0.715 *mm* +/- 0.010	0.502 *mm* +/- 0.008	0.426 *mm* +/- 0.006
Scintillation	0.0017	No Data	0.0155	0.0204	0.0319

Table [3.2] A summary of the fitted scales corresponding to the correlations shown in Fig [3.5]. The scintillation is a measure of the ratio of the standard deviation of the signal to the mean signal.

Several points should be very strongly emphasized from this data. The scales measured get smaller as *Re* increases and the scales measured are comparable to measures of the Kolmogorov microscale as reported by other researchers who used hotwire anemometry to investigate similar flows (see table 3.4). All small turbulent scales would be expected to get smaller as *Re* increases and the correlation curves reflect this. Second, as Re increases, the error bars get smaller and the scintillation increases. This is also what would be expected. Stronger turbulence implies more numerous smaller scales that dissipate more energy to heat. Those structures will

produce more scattering in comparison to the structures in a slug of air produced by more placid conditions. The scintillation for still air represents a certain noisy baseline voltage fluctuation as ultimately input into the computer. The largest source of this noise is likely the noisy three bits on each channel of the DAQ. For turbulent flows, the scintillation is more than an order of magnitude larger than it is for still air.

As noted before however, a horizontal correlation, in the direction of the flow allowed same slug of air to blow from the view of detector A to the view of detector B. One would expect this could make a false contribution to correlation length measurements by slightly increasing them. This is what was observed. Local isotropy in fully developed turbulence is assumed. A vertical displacement of the detectors would be expected to give spatial data just as theoretically relevant. However, it would not suffer from any possibility of the same slug of air being registered by both detectors.

This effect is clearly seen in fig [3.6]. The characteristic length scale of this flow was determined to be close to 0.5mm. The first step of the horizontal displacement decreases markedly less than the vertical displacement does over an interval of 0.5mm. However, the two curves overlap significantly more at greater displacements since they are larger than the characteristic scales of the flow, and a pattern seen at detector A will not have the ability move in time to be seen at all by detector B in the time interval of one cycle of the correlation calculation.

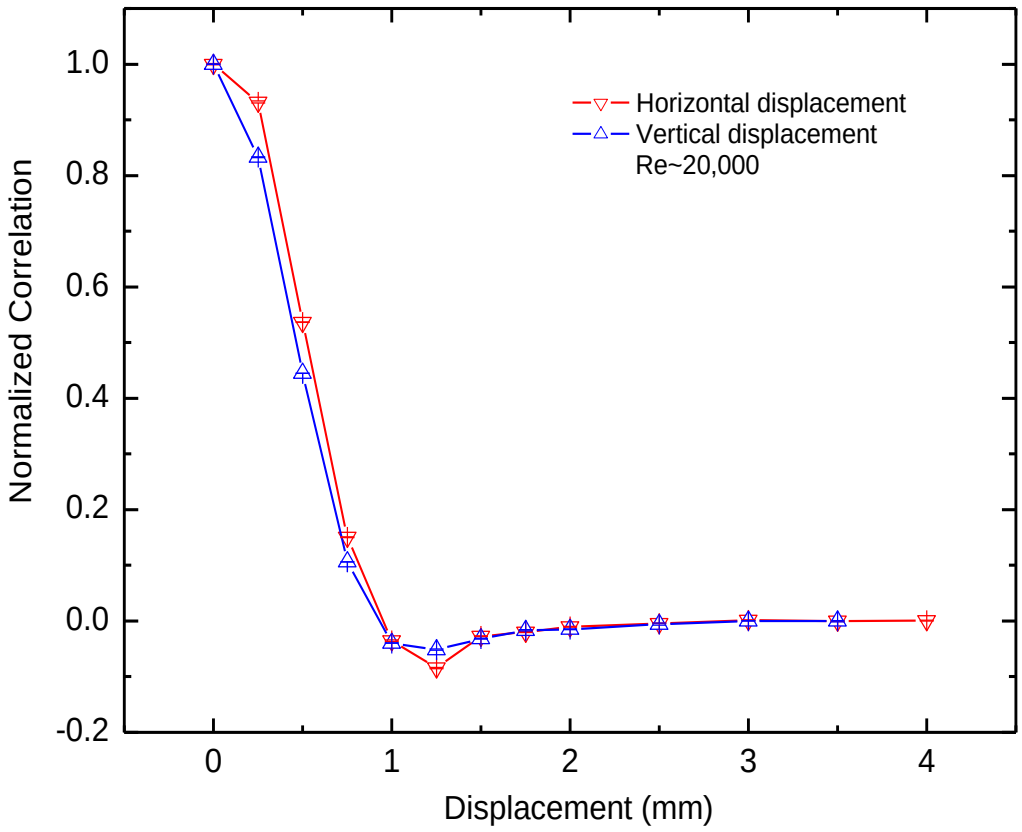

Fig[3.6] Horizontal (streamwise) vs. Vertical displacement in comparison for the same flow. Individual data runs were taken for four minutes instead of the normal three.

All subsequent data was taken with vertical displacements. In order to make the best possible fit to the initial decay in correlation, the first four data points of each set were fit with a Gaussian. This was justified since the correlations were always close to zero at a 1 mm separation. Fig[3.7] is an example of such a fit.

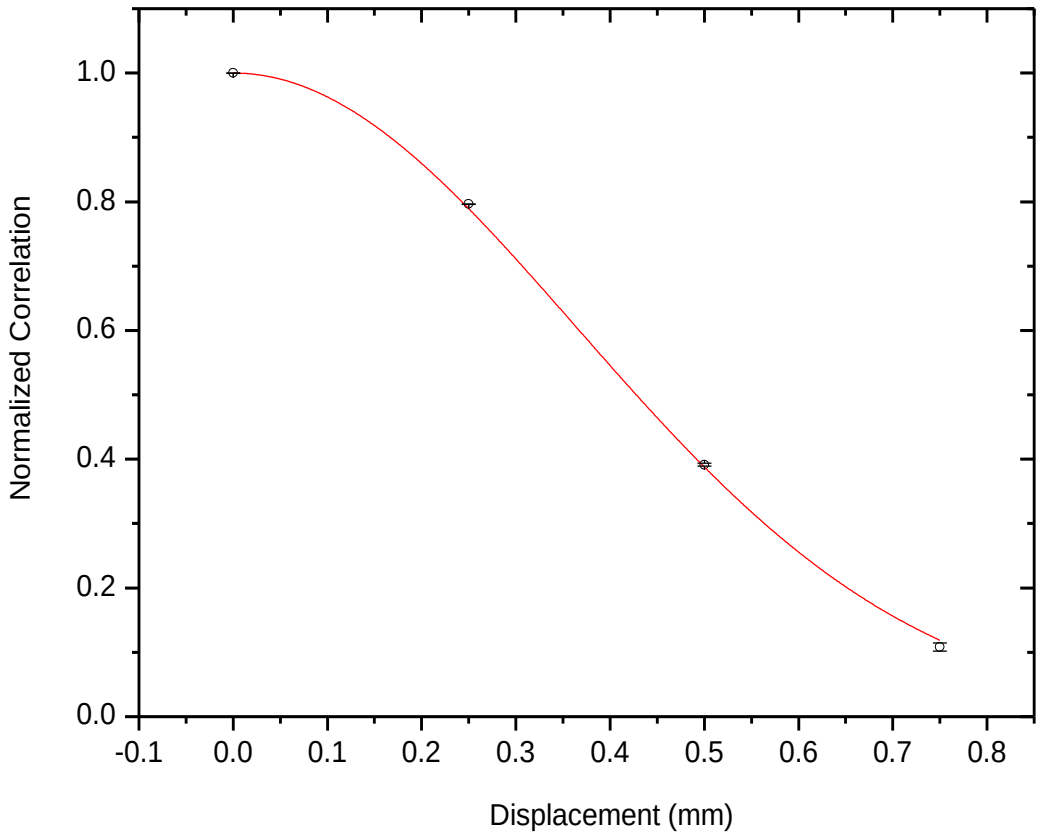

Fig [3.7] A representative Gaussian fit to the vertical data. In this case, the displacement is vertical and the flow is Re ~ 24,800, T = 88 C and the beam axis is 60 cm from the mouth of the blower.

It is expected that different parts of the flow would demonstrate different characteristics. The initial vorticity generating disturbances are primarily caused by the grid over the mouth of the blower. Close to the mouth of the blower, that vorticity has not yet had the chance to diffuse through the flow. Due to this one would expect the small scales to be smaller on average than further down stream where the full turbulent cascade has had a chance to develop. This effect was also observed.

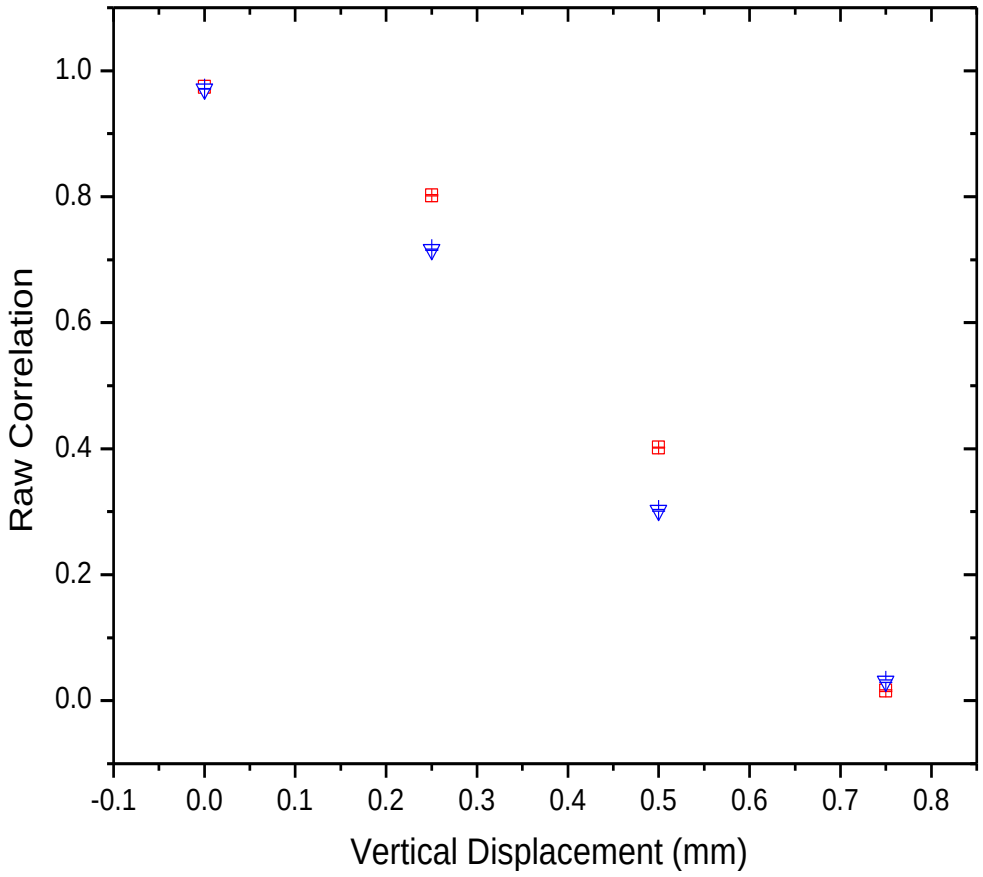

Fig [3.8] Triangles represent data taken with the beam axis 30 cm from the mouth of the blower. Squares were taken at a 60 cm beam distance. The same flow was used for both data sets. Re ~ 24,800 and T = 88 C.

The results of the vertical data runs are collected in table [3.3].

	u = 8.7 *m/s* *T* = 88 *C*	*u* = 10 *m/s* *T* = 88 *C*	*u* = 12 *m/s* *T* = 88 *C*	*u* = 12 *m/s* *No Heating*
Re	~ 18,000	~ 20,000	~ 24,800	~ 24,800
Gaussian Width (60 cm)	0.446 *mm* +/- 0.026	0.395 *mm* +/- 0.029	0.320 *mm* +/- 0.008	0.349 *mm* +/- 0.005
Gaussian Width (30 cm)	0.370 *mm* +/- 0.016	0.361 *mm* +/- 0.018	0.357 *mm* +/- 0.022	No Data

Table [3.3] Collected results for data taken with vertical displacements and the beam axis at distances of 30 cm and 60 cm from the mouth of the blower. No heating denotes a run done without using the heater. The device can see turbulent structures even without extra heat as a decoration.

As was noted in the first chapter, as *Re* increases, the small scales of turbulence become smaller. Clearly the hot plate was a source of convective turbulence to the flow. The "no heat" data, shows that for the same blower settings at *Re* ~ 24,800 the scales were larger than those in the same flow with a convective heat contribution added. What is striking is that the heating adds a comparatively small effect to high *Re* flows. The flow with *Re* 20,000, yet full heating, has scales which are greater in size, in comparison to the non heated data at *Re* 24,800 than that data is in comparison to the heated *Re* 24,800 data. It is important to stress that the device can detect small turbulent scales without having to heat the flow first. The use of the device has a much broader range of applicability than it would otherwise.

The next question to be addressed is of which small scales the device is measuring. From the start, the scales are much smaller, by two orders of magnitude, than any reasonable estimate of the outer scale of the system which is on the order of centimeters. The outer scale here is estimated to be 34mm and is the same dimension used in the approximation of *Re*. The next scale down, that is commonly measured, is the integral scale, which as discussed, is in effect a weighted average (by population) of all the scales in the inertial convective range. This too would be expected to be on the scale of centimeters for flows like the ones examined. The scales measured are small. The question becomes, are they comparable to the Taylor scale, the Kolmogorov microscale or somewhere between?

To answer this, a literature search for other flows which were measured by hotwire probes was performed, and our own hotwire measurements were made.

Hotwire Anemometry

Mouri, Hori and Kawashima [24] made wind tunnel measurements of grid generated turbulent scales, in flows similar to ours, with hotwire probes. Zhou, Antonia et al. report a range of λ of 3.1mm – 6.7mm and a range of η of 0.21mm – 0.49mm in a grid turbulence experiment with similar conditions to ours.[25]

u (m/s)	9.37	8.33	8.82	12.4	12.6
d (m)	2.0	3.5	8.0	3.5	8.0
λ (mm)	4.85	7.13	10.2	5.59	8.24
η (mm)	0.208	0.242	0.327	0.177	0.245

Table [3.4] Data taken from Mouri, Hori and Kawashima [24]. The parameter d is the distance of their probes from the grid.

In these experiments, the Taylor scale is an order of magnitude greater than the Kolmogorov microscale. However, the reported values of the microscale fit the ranges of our optical experiment very well. As remarked earlier, one would expect the smallest scales to scatter the most and produce the strongest signals.

The last step in answering which scales exactly were observed came from attempting to make our own hot wire experiments. As remarked earlier, the Taylor scale is extracted from hot wire data via the x intercept, of a parabola created from the first two terms of the Taylor expansion of a fit to the spatially transformed correlation

data from a hotwire probe. The run shown here was for a Re 24,800, T = 88 C data set, with the hotwire probe displaced 60 cm from the mouth of the blower.

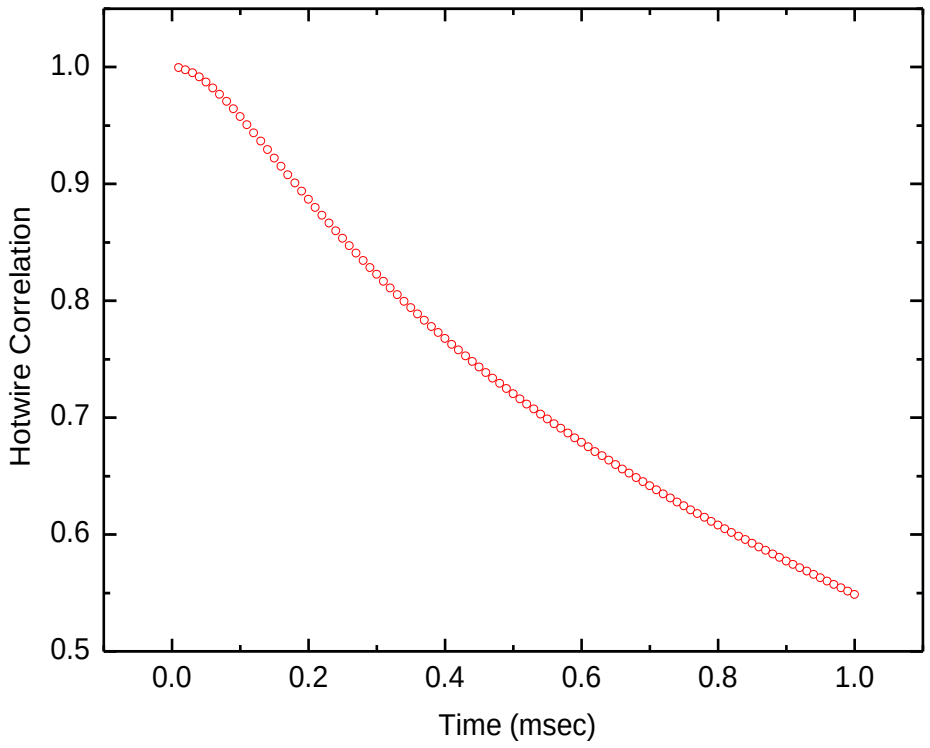

Fig [3.9] Hotwire data for a Re 24,800, T = 88 C flow at a beam displacement of 60 cm. Local flow speed was 7.1 m/s. Run time was 3 min. Sampling was done at 100 kHz. Error bars are suppressed.

Analysis of this data reveals one of the key results of this research. For this flow, $\lambda = 3.67\,mm$ and $\eta = 0.34\,mm$. In comparison, the Taylor scale measured with the hotwire probe corresponds well with the hotwire work of others and the optically measured width for this flow, using our device (as measured by a vertical displacement) was 0.320 *mm*! While it is likely that the closeness of this match is serendipity, from this and other considerations, it seems very likely that the scales being directly measured by the optical probe are indeed the Kolomogorov microscale.

As a final remark on our results, the apparatus was mounted on mobile optical breadboard that was affixed to a tripod. Data were collected during several days over the summer over a path of 100 ft. The beam axis was approximately 1.5m over a sidewalk. It was felt that convective rolls off of the sidewalk coupled with gusts of wind would produce a strong optical turbulence. We were not disappointed. Unfortunately, unless conditions were exceptionally placid, it proved impossible to create reproducible results. Over the course of a single three minute run, conditions could change substantially. If the day was gusty, it was even impossible to reproduce results from one run until the next with 30 second runs. Beam wander was also a major issue. This technique is not effective at long range in the regime where most optical experiments in this field are performed.

Closing Remarks, Conclusions, and the Future

A new device which can observe the smallest scales in clear air turbulence was created and demonstrated to probe the smallest scales of turbulence in a robust manner. There are many directions that the development of this device could go. One could imagine, instead of using only two detectors using a bank of detectors arrayed horizontally and vertically. In principle, the entire spatial correlation function could be taken at once. Even without going to that length, simply automating the translation of the detectors and data acquisition could make this device much more easy to use.

As it is though, it is substantially easier to set up and operate than a hotwire probe. It very quickly produces extremely accurate results without disturbing the flow in any way, or requiring the addition of any sort of tracer particle. In any fluid application where there would be interest in the smallest scales of turbulence, such a device could find a use.

There are numerous theoretical questions that need to be explored. The nature and origin of the negative portions of the correlation functions is an obvious place to start. The correlation functions produced certainly contain much more information than simply the width of a fitted Gaussian. Even though certain two point velocity field correlations as measured by multiple hotwire probes, do go negative, and have shapes very similar to the correlations seen here [26]. It is not yet clear exactly how those correlations relate to the optical correlations. However tempting it may be to claim the two have a one to one correspondence, or even a direct proportionality to each other, more study needs to be done before such a claim can be made.

A promising potential application of this device might be to exploit its ability to recognize different flows, in real time, and hence provide greater safety for aircraft. Turbulent conditions on runways are a dangerous cause of accidents for many small aircraft. A version of this device could be set up at the end of a runway sufficiently far enough back where it would not be likely to be hit by aircraft which were taking off or landing. The entire set up could fit within a square meter. With sufficient data collection to create profiles of dangerous conditions to compare measured

correlations against, this instrument could be used as a warning device to wave off aircraft when conditions were unsafe.

Appendix

The Labview code. The diagram begins on the next page, continues on the page after and flows from top to bottom in its current alignment.

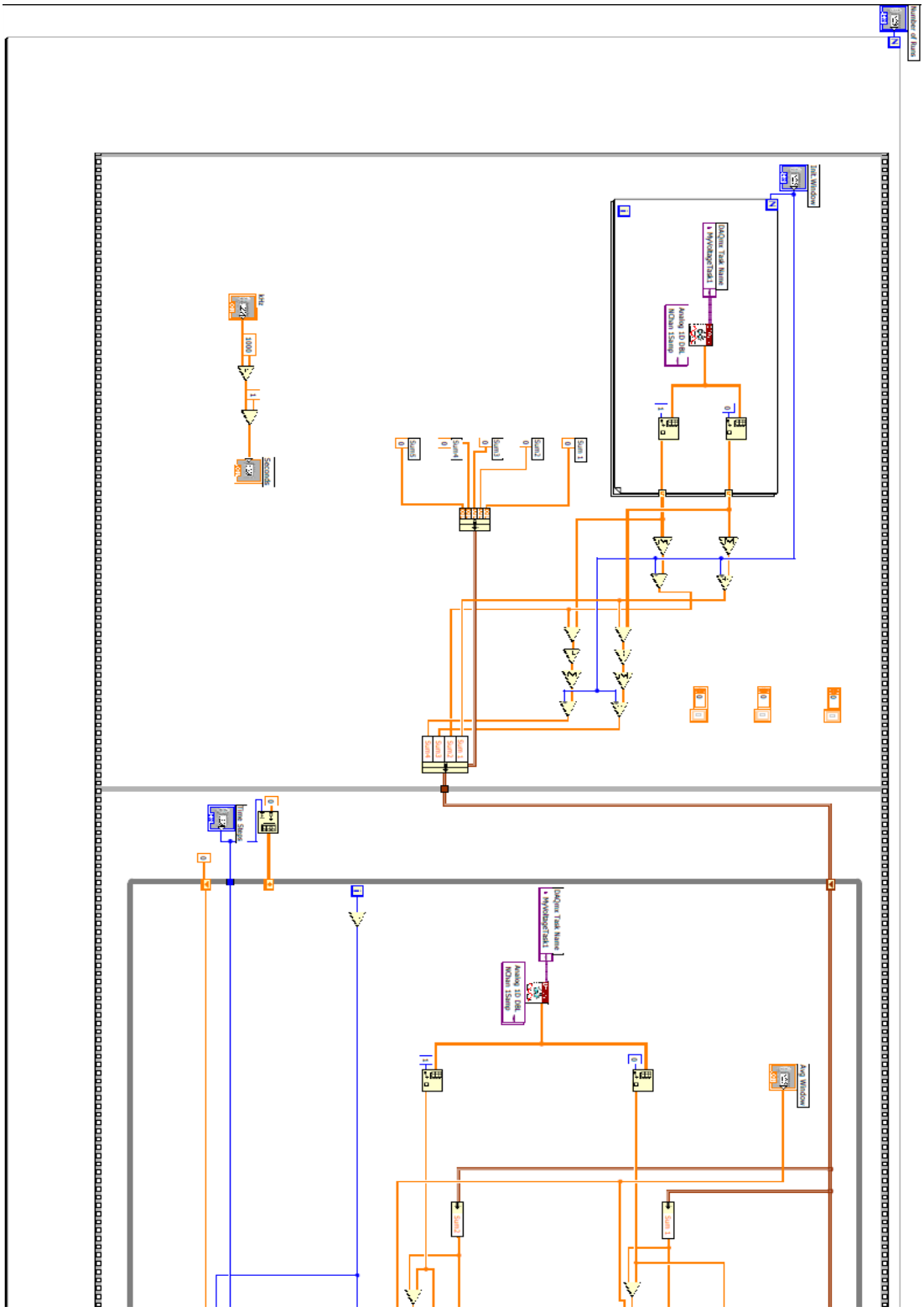

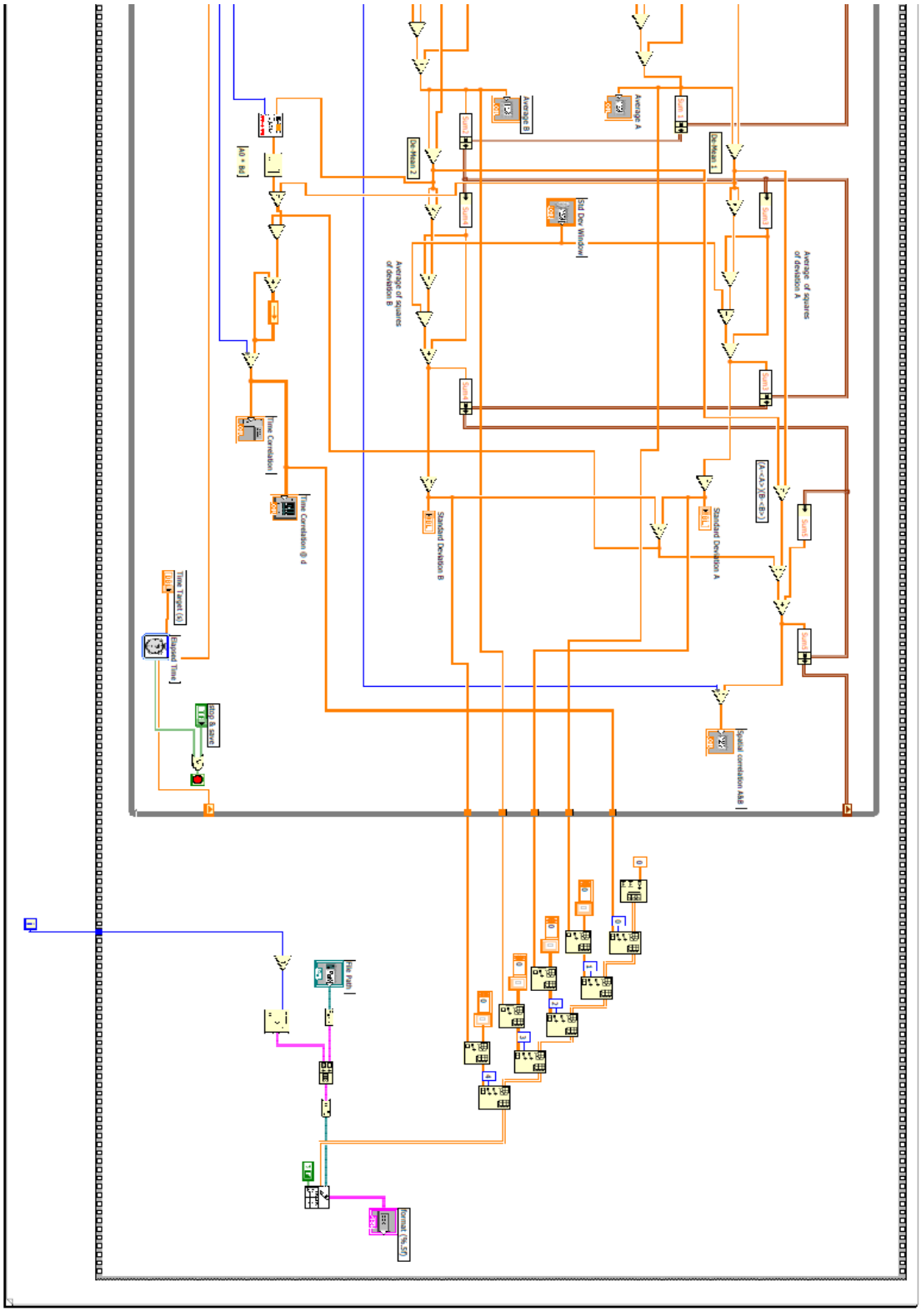
Average A
Average B
Sum
Sum 1
Sum 2
Sum 3
Sum 4
Sum 5
Sum 6
Sum 7
Sum 8
Sum 9
Sum 10
Sum 11
Sum 12
Sum 13
Sum 14
Sum 15
Sum 16
Sum 17
Sum 18
Sum 19
Sum 20
Sum

Bibliography

[1] L.D.Landau, E.M. Lifshitz, *Fluid Mechanics*, Pergamon Press, 1959.

[2] P.A. Davidson, *Turbulence, An Introduction for Scientists and Engineers*. Oxford University Press, 2004.

[3] V. I. Tatarskii, *The Effects of the Turbulent Atmosphere on Wave Propagation.* IPTS, Jerusalem, 1971.

[4] J. O. Hinze, *Turbulence, An Intorduction to Its Mechanism and Theory*. McGraw Hill Book Company, NY 1959.

[5] A. Tsinober, *An Informal Introduction to Turbulence,* Kluwer Academic Publishers, Dordrecht, The Netherlands, 2001.

[6] U. Frisch, *Turbulence.* Cambridge University Press, 1995.

[7] K. R. Sreenivasan "Fluid Turbulence" *Rev. Mod. Phys*, (1999) Vol. 71, No. 2, Centenary pp.383-395.

[8] A.N. Kolmogorov, *Proc.R.Soc.Lond. A*(1991) **434**, 9-13[Doml.Akad.NuakSSSR(1941)**30**(**4**)].

[9] A.N. Kolmogorov, *Proc.R.Soc.Lond. A*(1991) **434**, 15-17[Doml.Akad.NuakSSSR(1941)**32**(**1**)].

[10] K. R. Sreenivasan and R. A. Antonia "The phenomenology of small scale turbulence" *Annu. Rev. Fluid Mech.* (1997) Vol. 29 pp. 435–472

[11] K. P. Zybin, V. A. Sirota, A. S. Il'in, and A. V. Gurevich "Generation of Small-Scale Structures in Well-Developed Turbulence" *Journal of Experimental and Theoretical Physics* (2007) Vol 105, No. 2, pp. 455–466.

[12] R. A. Antonia, A. J. Chambers, D. Britz and L. W. B. Browne "Organized structures in a turbulent plane jet: topology and contribution to momentum and heat transport" *J . Fluid Mech*. (1986), Vol. 172, pp. 211-229

[13] V. A. Banakh, I. N. Smalikho and C. Werner "Numerical simulation of the effect of refractive turbulence on coherent lidar return statistics in the atmosphere," *Applied Optics.* (2000) Vol. 39, No. 30 pp. 5403-5414

[14] L. Andrews, R. Phillips, *Laser Beam Propagation through Random Media* SPIE,Washington ,1998

[15] R. J. Hill, and S. F Clifford "Modified Spectrum of the Atmospheric Temperature Fluctuations and its Application to Optical Propagation", *J. Opt. Soc. Amer*. (1992) Vol. 68, pp. 892–899

[16] M. Manning, *Stochastic Electromagnetic Image Production* McGraw-Hill, NY, 1993

[17] J.D. Jackson, *Classical Electrodynamics*, John Wiley and Sons, 1999

[18] R. L. Phillips and L. C. Andrews, "Measured statistics of laser-light scattering in atmospheric turbulence," *J. Opt. Soc. Am.* (1981) Vol. 71, pp.1440-1445

[19] L. C. Andrews, R. L. Phillips, C. Y. Hopen, M. A. Al-Habash "Theory of optical scintillation" *J. Opt. Soc. Am. A* (1999) Vol. 16, No. 6

[20] C. C. Cheng and M. G. Raymer "Propagation of transverse optical coherence in random multiple-scattering media" *Phys. Rev. A* (2000) Vol. 62, 023811

[21] R. J. Hill, "Review of Optical Scintillation Methods of Measuring the Refraction Index Spectrum, Inner Scale and the Surface Fluxes", *Wave. Random Media 2*, (1992) pp. 179–201.

[22] J. H. Churnside, "A Spectrum of Refractive Turbulence in the Turbulent Atmosphere", *J. Mod. Opt.* (1990) Vol 37, pp. 13–16.

[23] S. Bernard and J. M. Wallace, *Turbulent Flow Analysis, Measurement and Prediction*, John Wiley and Sons, 2002

[24] H. Mouri, A. Hori Y. Kawashima "Vortex tubes in velocity fields of laboratory isotropic turbulence:Dependence on the Reynolds number" *Phys. Rev.E* Vol. 67, 016305 (2003)

[25] T. Zhou, R. A. Antonia, L. Danaila, F. Anselmet
"Transport equations for the mean energy and temperature dissipation rates in grid turbulence" *Experiments in Fluids* (2000) Vol. 28 pp.143-151

[26] H. L. Grant "The large eddies of turbulent motion" *J. Fluid Mech.* (1958), Vol. 4 pp. 149-190

[27] V.I Tatarskii "Use of the 4/5 Kolmogorov equation for describing some characteristics of fully developed turbulence" *Physics of Fluids* (2005) Vol. 17, No.3 art. 035110

[28] U. Frisch "From global scaling, a la Kolmogorov to local multifractal scaling in fully developed turbulence" *Proc. R. Soc. Lond. A* (1991) Vol. 434, pp. 89-99

[29] R. L. Fante “Electromagnetic Beam Propagation in Turbulent Media” *Proc. IEEE* (1975) Vol 63, No. 12 pp. 1669-1692